ELUCIDATION OF CRITICAL RESIDUES WITHIN THE EXTRACELLULAR LOOP OF THE EPITHELIAL SODIUM CHANNEL

by

Kimberly J. Ramsdell, B.S.

A Thesis submitted to the Graduate Council of
Texas State University in partial fulfillment
of the requirements for the degree of
Master of Science
with a Major in Biochemistry
December 2016

Committee Members:

Rachell Booth, Chair

Karen Lewis

L. Kevin Lewis

FAIR USE AND AUTHOR'S PERMMISSION STATEMENT

Fair Use

Duplication Permission

ACKNOWLEDGEMENTS

I would like to begin by thanking Dr. Rachell Booth for all her time, guidance, and encouragement throughout this journey. When searching for a lab to work in for my Masters I interviewed with many professors on campus. I was interested in many of their research topics, but when I met with Dr. Booth I felt a connection on a more personal level. She was not only interested in my academic background, but also interested in who I was as a person and what I wanted from life as a whole. Coming back to college after a stint in the working world gave me different goals and motivations for my degree seeking than many students in my cohort. I knew what it was like in the real world and understood that obtaining my degree would be the best way to equip myself for the next steps in life. I came back to school knowing that I would work very hard for two years, obtain a job in the scientific field, and then begin the journey of building my family with my husband by planning our first child. Dr. Booth was the only professor I interviewed with who I felt comfortable enough to tell of my plans to start a family after my degree. She has been an inspiration on so many levels. Observing a brilliant, loving, hard-working, caring, and determined mother of three be so successful and involved in the scientific community has really helped me dream big and work hard to accomplish my goals. She is living proof that you really can do it all if you put your mind to it. Thank you so much for all you have instilled in me. You have made a lasting impact on my life.

Secondly I would like to thank my husband Aaron for being there for me through this journey. He has been my biggest supporter and my rock through these difficult two years. He has been there to celebrate my successes and has supported me through my hardships. He has pushed me to continue working hard, even when experiments are not working out, and encouraged me to never settle for anything less than my best. He listens to me babble on in science speak and has the patience and inquisitiveness to not

only listen, but to ask questions that engage my thinking and allow me to work through the puzzles that some experiments have presented. He has put up with a crazy schedule and not being able to spend a lot of time together while continually supporting me working for my dreams. I truly do not know how I could have done this without his love and support. Thank you, I love you more and more every day!

I also want to thank my parents, family, and friends for all their encouragement along the way. My parents have been so incredibly supportive, both emotionally and financially, and I find myself pushing harder to accomplish my goals because I want to make them proud. I am so lucky to have them and wouldn't be where I am today without their love and support. I have sacrificed a lot of personal time during this journey to get the most I can from this experience. I've missed birthdays, anniversaries, holidays, births, funerals, and many other social events along the way and I know it has been hard for many that I love. But thankfully I have the best support system and they have all been so understanding and encouraging. Thank you all so much for having my back and being patient and accepting about how I spend my time. I have had so much love and reinforcement from family and friends I truly know that I am blessed to have you all!

Finally I would like to thank my professors and collaborators for all the help along the way. Dr. Karen Lewis has always been there to help me trouble shoot problems, brainstorm new ideas, and has allowed the use of tools and equipment needed for my investigation. Her enthusiasm for her work and her endless encyclopedic knowledge has been an ever inspiring presence over the past two years. Dr. Ron Walter took me under his wing encouraging my hard work ethic and shifting my scientific approach from focusing on individual experiments to always keeping in mind the overall picture and story being told. He also helped me become more independent in my research by encouraging me to search for solutions to my problems utilizing any tool necessary before I go and ask for answers. I also want to thank Dr. Nina Boiko of the

Dr. Jim Stockand lab at the University of Texas Health and Science Center in San Antonio, TX for her time conducting the mammalian electrophysiology studies.

Last but definitely not least I would like to thank my fellow students and lab mates Olivia Kreidler, Chance Berman, Jose Castro, Eliseo Salas, Jordan Chang, Eleute Pena, Esther Lee, and Daniel Horn for everything they have done to help me keep my sanity throughout this journey. You have all made an impact on my success and I greatly appreciate who each of you are as individuals and as scientists. I feel so incredibly lucky to have found so many wonderful, smart, and encouraging individuals to call friends and colleagues. Thank you to everyone who has been on this crazy ride with me. You have all had a great deal to do with my success and it will never be forgotten.

TABLE OF CONTENTS

Page

LIST OF FIGURES

Figure **Page**

ABSTRACT

The epithelial sodium channel (ENaC) is a membrane protein complex located in the distal tubule of the nephron in the kidney which is responsible for the reabsorption of the final 3-5% of sodium from the urine back into the blood. ENaC is a constitutively open ion channel located in the apical membrane of epithelial cells which works in conjunction with sodium/potassium pumps and aquaporins to regulate ion concentration and fluid balance within the blood. Genetic disorders that cause mutations in ENaC have been correlated to imbalances in blood pressure making it greatly important to study the structure of this protein as it relates to function. This investigation aimed to elucidate critical residues within the ENaC extracellular loop that are critical for optimal functionality. To identify critical residues, previous work was conducted to induce random mutations through the use of error prone PCR. Mutant genes were transformed into yeast cells and preliminary functional screens were conducted. Analysis of previous yeast screening was conducted and mutants of interest were selected for further study. For this investigation, the mutant genes of interest were transformed into *Saccharomyces cerevisiae* yeast strain S1INsE4A and subjected to a novel yeast screen to observe changes in protein function based on growth inhibition. Mutant gene products exhibiting changes in functionality when compared to wild type ENaC were then sequenced and characterized based on number and location of point mutations and changes in amino acid sequence. Mutants containing single amino acid changes leading to an increase in

ENaC function in yeast screenings were cloned into a mammalian vector. Chinese hamster ovary cells were transfected with mutant vectors and subjected to electrophysiological studies to see if increased ENaC functionality was also exhibited in this model system. The correlations of functional change in ENaC in both model systems support that the position at which the amino acid changes occurred were critical to proper ENaC function.

I. INTRODUCTION

Vertebrate organisms maintain homeostatic osmotic pressure and electrolytic balance in extracellular fluids through well-regulated processes that utilize water and salt transport across cell membranes (1). Sodium (Na^+) is one of the most crucial cations within this extracellular fluid. The amount of Na^+ in the body is directly correlated to fluid volume, making Na^+ a key regulator of blood pressure (2). When changes in ion concentration occur, it leads to changes in fluid volume of the blood which can cause either hypertension (increased volume and pressure) or hypotension (decreased volume and pressure) within the vascular system. Hypertension has been reported as the most common human disease, affecting over 1 billion people worldwide. It is a treatable condition that a contributor to other life limiting ailments including; heart failure, kidney failure, myocardial infarction, and stroke (3). The American Heart Association reports an estimated annual cost of treatment for cardiovascular disease and stroke alone equaled $320.1 billion in 2011. This has been reported to be the highest cost of any other diagnostic group which makes hypertension both an economically and medically relevant issue for today's society (4). Of the many regulatory mechanisms that function in vertebrate organisms to maintain homeostatic electrolyte concentration, proper functioning of ion channels is of primary importance.

Ion Channels

Ion channels regulate the movement of ions into and out of cells, and in this manner maintain the overall cellular fluid volume balance. The epithelial sodium channel (ENaC) is a passive amiloride sensitive ion channel that contributes to the maintenance of sodium concentrations and extracellular fluid volume by allowing transport of Na^+ across epithelial cell membranes. The movement of Na^+ across the membrane generates an electrical force that also facilitates the movement of an accompanying anion across the membrane (commonly Cl^-). The net transport of salt facilitates the osmotic transport of water, causing changes in extracellular fluid volumes (1).

ENaC ion channels are located within the apical plasma membrane of epithelial cells in various tissues throughout the body, and allow transport of Na^+ across tight epithelia (5). In humans ENaC is expressed in the colon, lungs, salivary glands, sweat glands, and in the kidney. In the colon, ENaC is responsible for maintaining ionic balance to regulate electrolyte loss through the stool. In the lungs, it regulates balance of the thick fluid layer necessary for clearance of mucus. In salivary and sweat glands ENaC functions to decrease luminal sodium and ensure excretion of low sodium saliva and sweat. This aids in maintaining Na^+ concentrations within the organism by preventing excessive electrolyte loss (6). ENaC channels are highly selective for Na^+ and lithium ions (Li^+), and show a much higher selectivity for Na^+ than potassium ions (K^+) with a Na^+/K^+ transport ratio greater than 500/1. This selectivity is based on ion size discrimination, with small monovalent ions such as Li^+, Na^+, and H^+ able to pass through the channel while larger ions (e.g. K^+ and NH_4^+) are excluded. Also, the ENaC channel is specific for monovalent cations. This selectivity has been attributed to the

diameter of the pore at its narrowest section. Large inorganic and organic cations have shown pore blocking ability since they may enter the channel opening, but are not able to pass through the channel at the narrowest section. Thus the narrow section of the ENaC pore is sometimes termed a “selective filter” that only allows small monovalent, positively charged ions to traverse the membrane (7).

ENaC in the Kidney

The role of ENaC in the kidney is of importance to this investigation. The effect of mutations in human ENaC proteins are most greatly exhibited when expressed in the kidney, with less effect on human health observed in mutated proteins expressed in other tissues (6). The movement of Na^+ through ENaC channels is passive, and relies on the maintenance of sodium gradients generated by the active transport of Na^+/K^+ ATPase pumps located in the basolateral membrane (1, 2, 5, and 7). ENaCs play a critical role in the nephron of the kidney (Figure 1) where they facilitate reabsorption of sodium and water from the urine back into the blood before final urinary excretion. ENaC shows varied expression in different parts of the distal convoluted tubule (DCT), connecting tubule (CNT), and cortical collecting duct (CCD) with higher expression observed in the outer membrane regions and lower expression in deeper tissues. Within the CCD, ENaC proteins are co-expressed with aquaporins that allow for changes in intercellular sodium concentration to be paralleled with osmotic movement of water to regulate fluid volume (7).

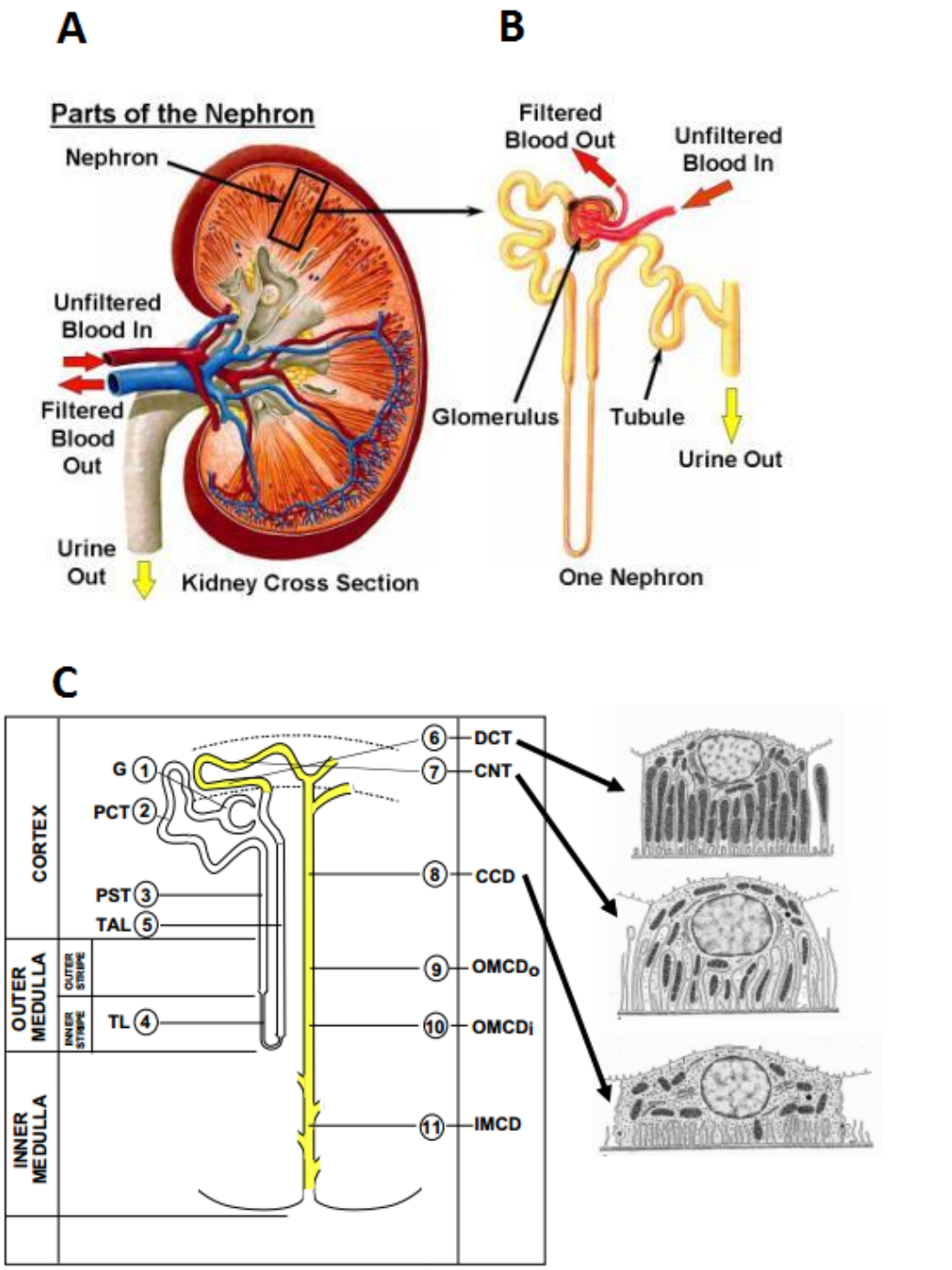

A,B: http://unckidneycenter.org/images/kidney-health-library-pictures/parts-of-the-nephron
C: Rossier,B.C. et al. FEBS Letters 587 (2013)

Figure 1: Transverse Cross-Section of the Kidney and Nephron Structure. A. Cross-section of the kidney highlighting the nephron. The kidney is responsible for filtration of the blood. B. Enlarged diagram of the nephron. The nephron is the basic functional unit of the kidney that contains ENaC channels. C. Nephron model diagramming important structural areas. ENaC reabsorption in the distal convoluted tubule (DCT) is of greatest importance to this investigation.

The first major step in the process of fluid filtration and reabsorption occurs in the glomerulus of the nephron, which functions to separate blood cells from the filtrate. The blood cells are then returned to the cardiovascular system and the filtrate travels through the remaining nephron. In humans, the glomerulus processes around 180 L of fluid. A large percentage of this fluid is reabsorbed in the distal sections of the nephron. The proximal tubule is responsible for the reabsorption of around 60%, the loop of Henle around 30%, and the distal convoluted tubule, connecting tubule, and collecting duct around 10%. The movement of filtered Na^+ ions from the urinary lumen of the collecting duct through the ENaC channel is the rate limiting step of the reabsorption process (5). After this process of reabsorption, only about 1.8 liters of urine is left to be excreted each day. The process of reabsorption is energetically costly, utilizing over 90% of the renal ATP through activation of Na^+/K^+ ATPases to maintain the Na^+ gradient needed to facilitate ENaC's passive transport (3).

Structure and Stoichiometry

ENaC proteins are members of the epithelial sodium channel/degenerin (ENaC/DEG) superfamily of ion channels which was discovered in the early 1990s (7). This superfamily includes ion channels that show a great degree of heterogeneity in functionality which is one of many unique characteristics of this ion channel family. The family functions include the maintenance of salt balance, mechanosensation, and sensory perception such as pain and touch. All channels whose function has been experimentally examined show selectivity for sodium, and varying sensitivity to the diuretic drug amiloride (see below) (2). Although the ENaC/DEG channels have a wide

range in function they possess highly conserved topological homology. The amino acid sequences are 15-20% conserved across the entire superfamily. Conserved membrane topology among superfamily members include cytoplasmic NH_2 and COOH termini and two transmembrane domains (M1 and M2) that are separated by a large cysteine-rich extracellular loop (Figure 2).

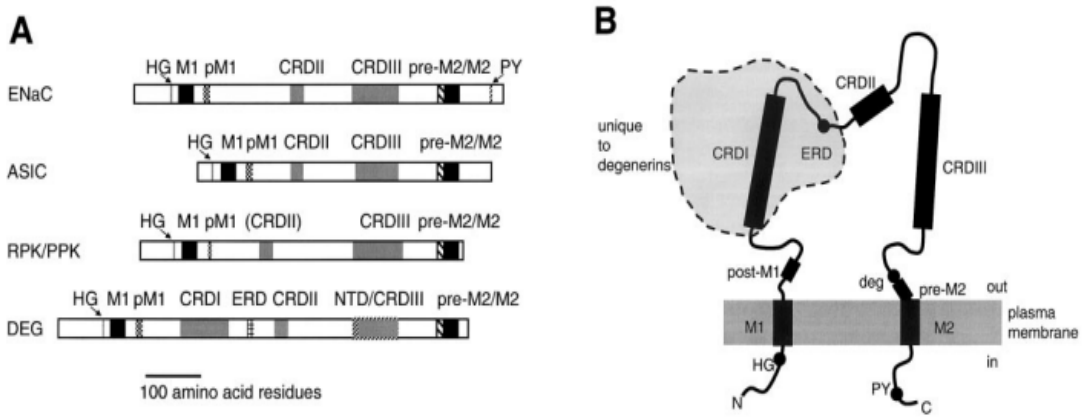

Kellenberger, S., and Laurent, S. Epithelial Sodium Channel/Degenerin Family of Ion Channels. Physiol Rev. (2002) 82:735-767

Figure 2: ENaC/DEG Family Conserved Domains and Genetic Localization. Membrane topology is highly conserved across the ENaC/DEG family. A. Conserved domains of subfamilies within primary structure with length of diagram domains representing relative size of domain within each protein. B. Diagram of conserved membrane topology.

The cysteine-rich extracellular loop is around 50 kDa (302 amino acids) and makes up more than half of the protein mass, which is another unique feature of the ENaC/DEG ion channel family. These channels also share several genetic motifs that are completely conserved, including the HG motif (His-Gly sequence on the NH_2 terminal very close to the M1), the RPxxTxC sequence following M1, the entirety of M2, and the cysteine rich domains (CRD) II and III of the extracellular loop. The superfamily is divided into three main subfamilies; (1) the ENaCs which share around 30% amino acid homology across the subfamily, (2) acid sensing ion channels (ASICs)

sharing 45-90% homology, and (3) the degenerins (DEGs) that show around 30% homology. Each subfamily exhibits its own gating mechanism.

The ENaC Ion Channel

The ENaC subfamily of ion channels is unique in being constitutively active and selective. ASICs are proton-gated channels that recognize H^+ as their gating ion; hence the name acid sensing ion channels (7). Degenerins rely on mechanosensitivity and require an external stimulus such as the stretch or tension within the lipid bilayer containing the channel. This is what allows degenerins to respond to external stimuli involved in touch sensitivity among other neuronal processes (2, 8)

Functional ENaC channels are protein complexes with varied combinations of three homologous subunits, alpha (α), beta (β), and gamma (γ) (Figure 3). Each subunit consists of a large luminal extracellular loop containing several functional domains, two transmembrane domains flanking the extracellular loop, and relatively short NH_2 and COOH cytosolic termini that follow a topological pattern used to classify the ENaC subfamily (2, 7, and 9).

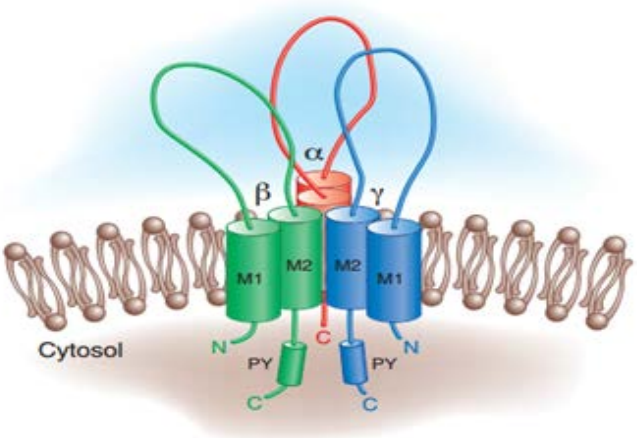

Bhalla, V., and Hallows, K. R. Mechanisms of ENaC Regulation and Clinical Implications. J Am Soc Nephrol (2008) 19:1845-1854

Figure 3: Proposed Structure of ENaC. ENaC is thought to express as a heterotrimer containing a single α, β, and γ subunits. Each subunit is composed of two transmembrane spanning domains, a large extracellular loop, and short cytosolic N- and C- termini.

ENaC genes have been cloned from many organisms including human, cow, mouse, rat, and *Xenopus*. Human and rat ENaCs exhibit around 85% amino acid similarity, making the rat an informative model for functional ENaC studies (7). Each subunit averages around 85-95 kDa in their unmodified form and share 30-40% amino acid similarity with the greatest genetic variation located within the extracellular loop domains (2, 5). ENaC subunits share conserved proline-rich motifs in the cytoplasmic (COOH) terminus, and the PPPxYxxL sequences are important for protein-protein interactions (7). Glycosylation, proteolytic cleavage, and other post-translational modifications can alter subunit size, and play critical roles in individual ENaC expression and functionality (5). Regulation of these processes is detailed later.

ENaC subunits can be separated into two main branches based on genetic location and similarity. One branch contains alpha (α) and delta (δ) subunits. Delta

ENaC is expressed within testis, ovary, and pancreas, with small amounts of expression in brain and heart where it has functionality similar to αENaC in kidney tissues. Since δENaC is not found within the kidney it will not be discussed further. The second branch of the ENaC subfamily contains β and γ ENaC. These ENaC subunits are not splice variants, but instead have their own genes (10). Alpha ENaC is encoded by the SCNN1A gene which is about 17 kb in size and located on chromosome 12. Beta ENaC and γENaC are encoded by the SCNN1B and SCNN1G genes, respectively, and are located in close proximity to one another on chromosome 16 suggesting they arose from an ancestral regional duplication. Each ENaC gene is comprised of 13 exons where exons 2 and 13 encode the transmembrane regions (7, 10)

Three ENaC subunits may form a homomeric complex (αααENaC only) or a heteromeric protein complex, consisting of differing stoichiometric ratios of three main subunits (α, β, γ) (11). The αENaC subunit can generate small amiloride-sensitive currents when expressed as a homomeric complex indicating this subunit as the crucial transporting subunit with β and γENaCs playing more of a regulatory role (7, 9). ENaC complexes containing a combination of the alpha subunit with either beta or gamma subunits have been shown to generate slightly greater currents than those generated by homomeric αααENaC (7). Bonny *et al.* (1999) concluded that minimal currents are detected when αβγENaC channels have a nonsense mutation ($\alpha_{R508stop)}$ in αENaC creating a predicted truncated alpha protein subunit close to the second transmembrane domain. This mutation is a characteristic of the genetic disorder pseudohypoaldosteronism (PHA1) (12) and suggests further studies are needed to also assess the effects of mutations in βγENaC on channel currents. Multiple studies have

been conducted by many research groups suggesting the most efficient functional complex is the trimeric αβγENaC (7, 9, 11, 13, and 14).

The true stoichiometric ratio of subunits within the αβγENaC channel complex remains unresolved. Studies conducted by Firsov *et al.* (1998) in *Xenopus* oocytes utilized antibody binding affinity functional assays to assess mutant subunit effects on interactions with channel blockers. These assays provided quantitative data for the relative abundance of each subunit within the functioning channel. The data suggested a tetrameric architecture based on two fold increased antibody signal for αENaC in comparison to β and γENaC subunits within the same channel. This ratio stayed constant upon overexpression of a single subunit. These data suggested a 2α:1β:1γENaC channel (14). However, the report of a 1:1:1 stoichiometric crystal structure of ASIC1, a closely related ENaC/DEG family member, by Jasti *et al.* (2007) now suggests a 1:1:1 structure for ENaC (Figure 4A). To confirm this, further experimentation must be completed (5, 15). Two slightly different but incomplete chicken ASIC crystal structures were also published. The first structure (PBD code: 2QTS) was a non-functional complex, likely due to removal of 25 residues from the NH_2 terminus and deletion of 64 residues from the COOH terminus (15). The second structure (PBD code: 3GHC) retained a small section of the NH_2 terminus that was truncated immediately proceeding the second transmembrane domain. This channel showed acid sensitivity and sodium selectivity, but had lower functionality than the wild type channel. These structures are similar homotrimers including full extracellular and transmembrane domains, and only differing in the composition of the intracellular termini (2).

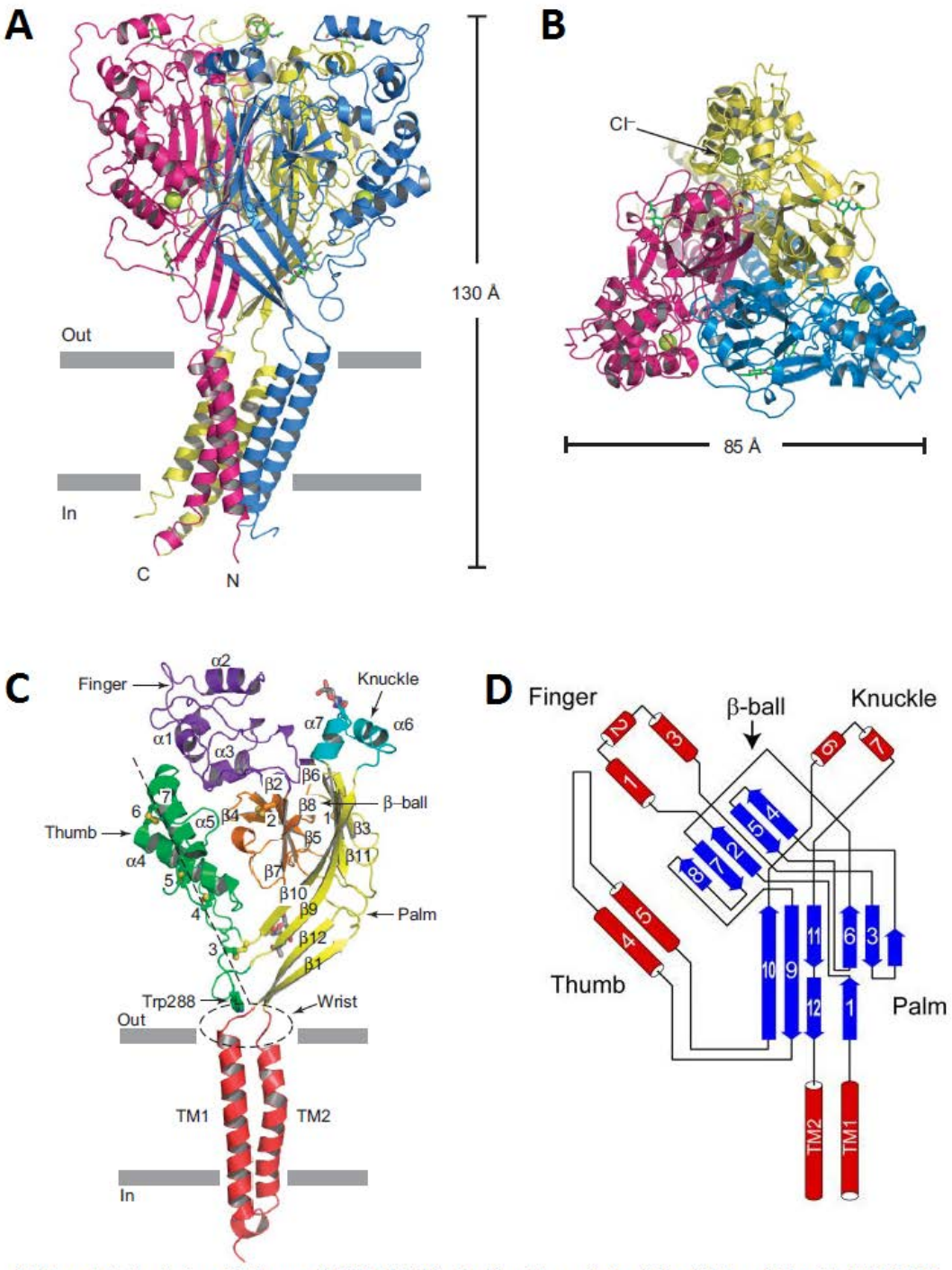

(A, B, and C): Jasti, J. et al. Nature (2007) 449. (D): Kashlan, D. et al. Am J Physiol Renal Physiol. (2011) 301

Figure 4: Crystallographic Structure of Chicken ASIC1. A. View of homotrimeric ASIC1 structure parallel to the membrane plane. B. View of homotrimeric ASIC1 structure parallel to the molecular three-fold axis from the extracellular side of the membrane. C. Domain organization of a single subunit with disulfide bridge locations. D. Topology diagram of ASIC1 α-helices (red cylinders) and β-sheets (blue arrows) with labeled domains.

The structure of ASIC presents a shape resembling an outstretched arm with a clenched hand holding a ball (Figure 4C, D). The higher order domains of the extracellular loop are assigned specific terms. The inner core contains the palm domain made of multiple antiparallel β-sheets closely associated with the β-ball domain containing smaller antiparallel β-sheets. This core structure of ASIC1 shares the 33-36% sequence identity with ENaC. The peripheral domains are the finger, thumb, and knuckle that are composed of α-helices and show much lower homology between ASIC1 and ENaC as well as high sequence variability among various ENaC subunits (2, 10, 15, and 16). The finger domain of ENaC contains many functionally relevant proteolysis sites that are thought to aid in regulation. Also, the orientation of this domain at the periphery is considered necessary for easy access to proteases and proper regulation (16). Proteolytic cleavage of ENaC subunits is one of many ways these proteins are chemically regulated.

Regulation

An understanding of ENaC regulation, although extensive, is not yet complete. The number of functional ENaC complexes at the cell surface appears to be a principal determinant of sodium regulation and fluid reabsorption. ENaC subunits are synthesized and modified within the endoplasmic reticulum where they are packaged for transport to the apical membrane. Post-translation N-linked glycosylation of the extracellular loop is an important step in this process (17). Several glycosylation sites exist for each subunit; 6 for αENaC, 12 for βENaC, and 5 for γENaC, however, only sites within the extracellular domain are utilized (7). Glycosylation allows for interactions with

chaperones (calnexin/calreticulin) that aid protein folding and protect conformational stability by guarding the extracellular loop core from proteolysis (17).

Response to chemical signaling is also an important regulatory process for ion channels. Members of the ENaC/DEG family show varying affinity for the diuretic, amiloride, which seems attributed to a highly conserved sequence of the pre-membrane spanning domain that contributes to the formation of the channel pore (7, 18). Identified by an extensive screening of over 25,000 compounds, amiloride functions to block electrogenic transport of sodium in cells (7). Amiloride is able to function as an ENaC pore blocker sub-micromolar concentrations resulting in decreased sodium conductance of apical tight epithelia. ENaC is unique among its superfamily due to its high affinity for amiloride (Figure 5A). Amiloride binds at the pore opening and interacts with specific residues within each subunit, αS583, βG525, and γG537 (Figure 5B). Kellenberger *et al.* (2002) showed that mutations in the conserved glycine regions of βG525 and γG537 decreased amiloride affinity 1,000 fold, while a mutation at αS583 only decreased affinity 20 fold. Glycine is conserved at homologous positions across the ENaC/DEG family suggesting the unique serine of the alpha subunit significantly contributes to the observed greater affinity seen in ENaC (7).

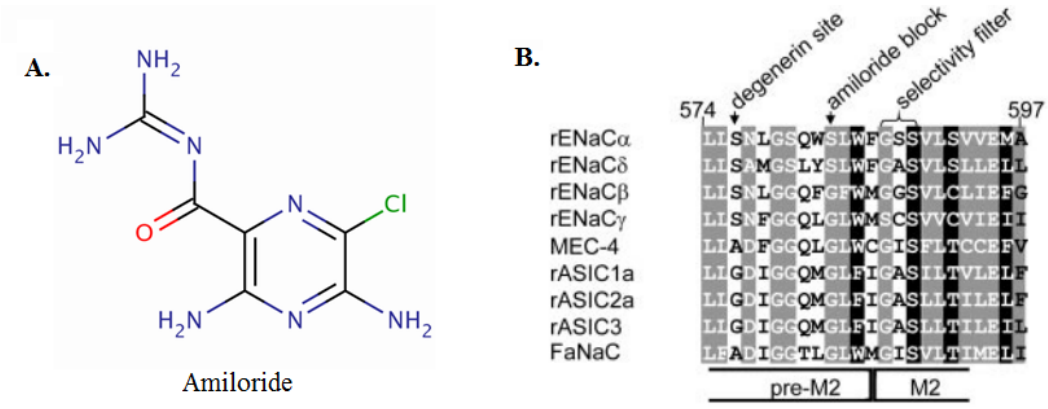

A. http://www.medicalook.com/reviews/Amiloride.html
B. Kellenberger, S. Gautschi, I., and Shild, L. Mutations in the Epithelial Na+ Channel ENaC Outer Pore Disrupt Amiloride Block by Increasing Its Dissociation Rate. Molecular Pharmacology. (2003) 64: 848-856

Figure 5: Amiloride Structure and ENaC Pore Region Sequence. A. Chemical Structure of amiloride. B. Pre-M2 and NH_2-terminal section of M_2 alignment of the ENaC pore region. The location of residues critical for amiloride block is shown. Black shading means 100% conservation, gray shading indicates 80% or greater conservation.

In contrast to the diuretic properties of amiloride, the antidiuretic hormone vasopressin can also have a major effect on ENaC regulation. Vasopressin binds to AVP receptor (V2) anchored in the basolateral membrane that activates adenylate cyclase and downstream production of cAMP. Cyclic AMP then activates recruitment of aquaporins (AQP-2) from intracellular space to the apical membrane (Figure 6) increasing membrane permeability to water molecules, concurrent with increase in ENaC activity and sodium reabsorption from the urine to the blood. This increase is rapid and can occur within minutes of binding to V2 (1, 7).

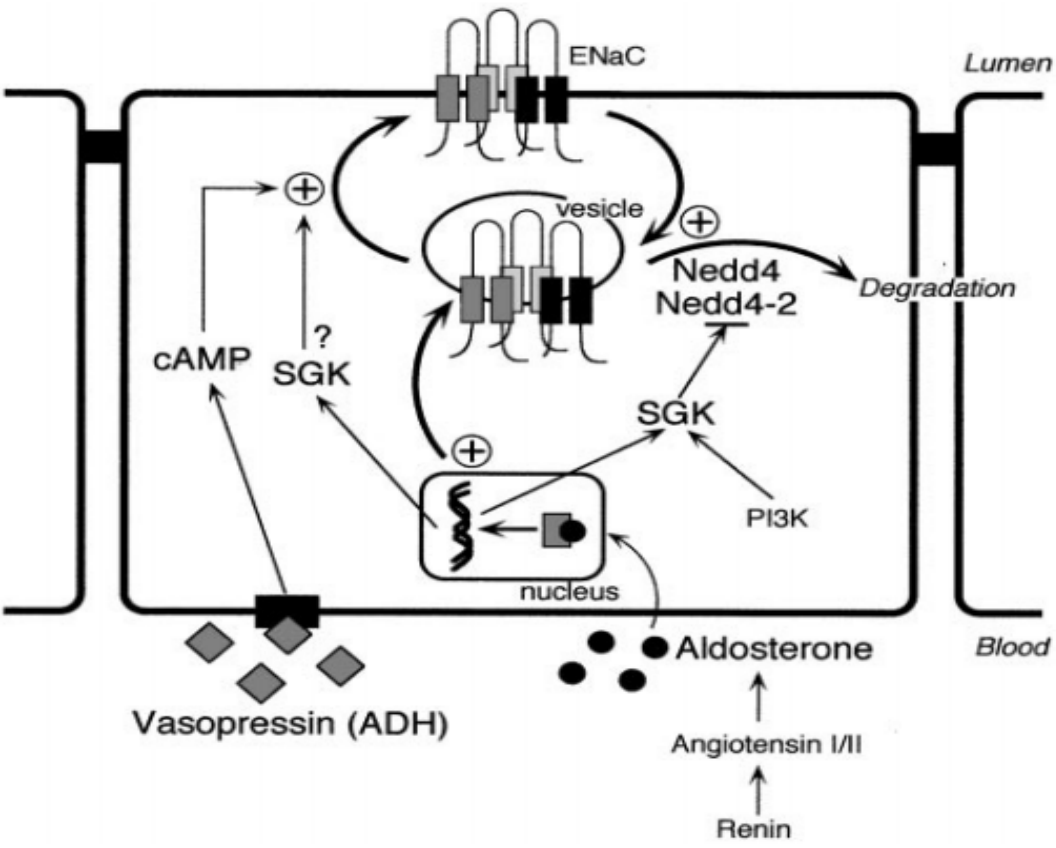

Snyder, M. P. The Epithelial Na+ Channel: Cell Surface Insertion and Retrieval in Na+ Homeostasis and Hypertension. Endocrine Reviews. (2002) 23(2)254-275

Figure 6: Regulation of ENaC Expression and Function at the Cell Surface. The function of many key regulators is diagramed here. Vasopressin and aldosterone act as ENaC activators, and Nedd4 is responsible for deactivation through ubiquitin tagging for degradation.

Another key regulatory element is the hormone aldosterone. Aldosterone regulates electrolyte metabolism in vertebrates (1). Aldosterone is a corticosteroid that is recognized by the mineral corticoid receptor (MR) expressed in the thick ascending limb, distal convoluted tubule, connecting tubule, and collecting duct of the renal nephron. The affinity of MR for mineralocorticoid is increased with the coexpression of 11β-HSD2. This enzyme metabolizes glucocorticoids into inactive metabolites, decreasing competition for the MR site. MR/11β-HSD2 co-expression regions include

the distal convoluted tubule, connecting tubule, and the collecting duct which together make up the aldosterone-sensitive distal nephron (ASND) (3). Aldosterone secretion is increased in response to decreased fluid volume (dehydration) as well as hyponatremia (low salt concentration in the blood). Aldosterone then binds MR and the hormone-receptor complex enters the nucleus where it acts as a transcription factor to directly increase αENaC expression by stimulating mRNA synthesis (Figure 6). The effects of aldosterone on sodium transport can be seen within 1-3 hours of binding to MR through an increase in the number of functional ENaC channels in the membrane as well as increasing the open probability within each channel (1, 7).

Aldosterone can also indirectly activate ENaC through interactions with other proteins involved in various kinase activated cascades. Aldosterone increases mRNA levels of the serum-and glucocorticoid-regulated kinase SGK (5, 7). SGK stimulates ENaC by increasing channel half-life through inhibition of channel degradation by Nedd4, another ENaC regulatory agent. Nedd4 is an ubiquitin protein ligase that attaches ubiquitin subunits to lysine residues at the NH_2 terminus, triggering protein degradation. Nedd4 is deactivated by phosphorylation by SGK that in turn decreases ubiquitination and ENaC degradation (Figure 6). ENaC activity may also be self-inhibited through negative feedback when external sodium concentrations are high (7, 9).

In addition to degradative processes, ENaC is also regulated via activation through specific proteolytic processing. The role of serine proteases to positively affect ENaC's ability to move salt has been well described. A number of proteases have been identified and their effects on ENaC characterized. Furin, channel activating protease (CAP2),

extracellular trypsin, elastase, and kallikrein are all proteases that have been shown to increase ENaC activity. Proteases can activate ENaC through direct cleavage of inhibitory sequences from subunits and can also indirectly increase activity. One example of indirect activation is prostasin, a proenzyme that requires post-translational cleavage by matriptase (CAP3) to activate ENaC (16).

ENaC subunits rely heavily on proteases for activation. Alpha and gamma subunits must undergo proteolytic cleavage to gain higher activity (17). Alpha and gamma subunits must be cleaved at two sites that excise a segment of amino acids. This suggests these amino acid sequences may serve an inhibitory function for regulatory processes. The alpha subunit contains two Furin cleavage sites and must be cleaved at both in order to become active. The gamma subunit has one Furin site and relies on prostasin to cleave at a secondary site releasing an inhibitory fragment to induce activation. It has been proposed these fragments constrain subunit movement around the thumb and finger domains of the extracellular loop, leading to the observed inhibitory effects. Functionality of these channels is decreased by 90% if not cleaved, 85% of this inhibition is attributed to the alpha subunit. This supports previous claims that gamma makes only a small contribution to channel activity. Rescue by introduction of trypsin suggests un-cleaved channels are localized to the membrane, but exist in a functionally inactive form (16).

Proteolysis is a very involved process requiring many different substituents and many different mechanisms to ensure activation of the channels. To answer the question as to why it is necessary for ENaC subunits to be processed by cleavage to induce activation Kleyman *et al.* (2009) proposed that these mechanisms evolved to allow

ENaC channels to be constitutively open. Within the ENaC/DEG family many proteins are intrinsically inactive and rely on external stimuli or ligand binding for activation. Proteolytic cleavage for activation provides an alternative mechanism to allow ENaC to be constantly active (16).

Genetic Disorders

Many regulatory pathways exist to maintain balanced ENaC function, but mutations of the ENaC sequences can alter the ability of these mechanisms to function optimally. Liddle's syndrome, also known as pseudoaldosteronism, is an autosomal dominant disorder which manifests in early onset hypertension (salt-sensitive), hypokalemia, and metabolic alkalosis. Cardiovascular and cerebrovascular symptoms can also manifest and are many times misdiagnosed (19). Mutations in the SCNN1B (β) and SCNN1G (γ) genes that lead to early termination and truncation of the COOH terminus have been found in this disorder (20, 21). Mutations in these subunits affect the PY motif in exon 13 and include missense, nonsense, and frame shift mutations. Twenty-two mutations have been characterized for this disorder, seventeen in β and five in γ (7, 19). ENaC channels expressing one or more of these mutant subunits show a gain of function when compared to wild type (22, 23). Gain in function mutations cause an increase in Na^+ reabsorption by increasing the number of functional ENaC channels localized to the membrane and increasing the channel's open probability (P_o) (19). This increase in ENaC reabsorption functionality increases the amount of sodium transported from the lumen of the nephron into the blood. Excess sodium in the blood then triggers the

movement of water into the blood through aquaporins increasing fluid volume and causing hypertension.

Pseudohypoaldosteronism type I (PHA-1) is another genetic disorder that manifests from its effects on ENaC but, in this case mutations lead to reduced channel activity or loss in function. Symptoms include hyponatremia, hypotension, and hyperkalemia (7). The genetic mutations identified in PHA-1 patients are recessive and may be categorized into four main types; premature stop codons (human αR56stop and αR508), frame shift mutations (αI68fr, αT168fr, αF453fr, βT216fr, βD305fr), missense mutations (αC133Y and βG37S), and an abnormal splice variant of γENaC at nucleotide 318 (7). Two forms of PHA-1 have been identified. Renal PHA-1 is associated with mutations of the MR, and systemic PHA-1 is associated with mutations within the subunits of ENaC (3). ENaC loss in function substantially lowers the amount of Na^+ reabsorbed from the nephron causing water to stay in and move to urine from the bloodstream. This causes a decrease in the pressure of the veins due to loss of water resulting in hypotension (23). Disorders such as Liddle's and PHA-1 rely on the understanding of ENaC structure and function for the production of effective treatments. The more that is known about the structure of ENaC, and its mechanisms of action, the better equipped the scientific community will be to then create novel therapeutics to ameliorate these conditions.

Elucidation of the structure/function relationships of ENaC subunits is critical to fully understanding the physiological, regulatory, and pathophysiological roles of this sodium channel. Further, understanding the mechanisms of action of ENaC can suggest novel treatments for diseases associated with ENaC dysfunction such as Liddle's and PHA-1. As stated, the extracellular domain shows low genetic conservation across the

ENaC/DEG superfamily and also shows high genetic variability between α, β, and γ subunits. Compared to the cytosolic termini and the transmembrane domains, very little is known about how the extracellular domains specifically affect ENaC functionality and regulation.

Project Goal

The epithelial sodium channel plays a key physiological role in the fine tuning of the concentration of sodium and fluid volume within the blood. Understanding the structure of this protein will lead to a better understanding of the function. The alpha subunit of ENaC has been shown to be the critical subunit for the function of the protein channel and is of great importance for further study. The goal of this project was to identify critical residues in the extracellular loop of the alpha ENaC subunit that are critical to the protein's structure and function. Previous work has been conducted in the Booth lab to induce random mutations in the extracellular loop domain of alpha ENaC through use of low fidelity error prone PCR. Preliminary functional studies in yeast containing homomeric alpha ENaC channels have been conducted and were studied to identify mutants of interest for further experimentation.

Mutants were characterized through further functional studies in yeast. Mutant plasmids from transformed yeast showing varied function be sequenced and aligned with wild type alpha ENaC to identify specific nucleotide mutations and changes in amino acid sequence. Mutants with minimal changes were further studied in yeast transformed with heteromeric ENaC channels.

Mutants that continue to be relevant after these experiments were cloned into a mammalian vector and transfected into mammalian cultures for electrophysiological studies. The mammalian electrophysiological studies were compared to the functional studies in yeast to identify similarities and differences between organismal systems. These studies will further support the findings that identified mutated residues used for yeast screenings are critical to proper functioning of ENaC.

II. MATERIALS AND METHODS

Plasmid DNA Isolation

Top 10 *Escherichia coli* samples were grown overnight at 37°C on LB plates supplemented with 100 µg/mL ampicillin. A single colony was selected from the plate and used to inoculate 5 mL of Luria-Bertani broth (LB) or Terrific Broth (TB) (also supplemented with 100 µg/mL ampicillin), and grown 12-24 hours at 37°C with shaking at 220 rpm. Plasmid DNA was isolated from these cultures using Qiagen QIAprep Spin Miniprep kit (Valencia, CA) following manufacturer's protocol. The protocol consisted of resuspending cells from culture, lysing the cells, neutralizing the reaction, separating the cell lysate from cell debris through centrifugation, binding plasmid DNA to a purification column, washing DNA with buffer solution, and then eluting DNA from the column using 50 µL of warm distilled water. Isolated plasmid DNA concentrations were quantified using the NanoDrop 2000 Spectrophotometer from Thermo Scientific (Waltham, MA) measuring absorbances at 260 nm and 280 nm. Plasmid DNA isolates were then analyzed utilizing horizontal gel electrophoresis. Isolates were stored at -20°C until further use.

Horizontal Gel Electrophoresis

Agarose powder (0.7-1.5%) was added to 1X TAE buffer (40 mM Tris, pH 8.0, 20 mM acetic acid, and 1 mM EDTA) and heated in a microwave in one minute intervals with swirling to mix until fully dissolved. The TAE/agarose was cooled at room temperature slightly before being poured into a gel caster, and then the well comb

was added. After solidifying (~30 minutes) the gel tray was removed from the cast and placed in a gel rig containing 1X TAE buffer. Samples were prepared by adding approximately 1 μg DNA, 1X loading dye, and deionized water to bring sample volume to 10-15 μl. Samples were loaded into the well of the gel and separated at 100 V for 70 minutes (voltage and time vary based on application) adjacent to an appropriate standard ladder. The gel was then rinsed with water and stained by adding approximately 0.2 mg ethidium bromide while agitating at room temperature for 15 minutes. The stained gel was then washed three times with deionized water while shaking for 5 minutes each. DNA fragments were then visualized with ultraviolet light on the ChemiDoc XRS+ Imaging System running Image Lab 5.1 software by Bio-Rad (Hercules, CA).

Transformation of Plasmid DNA into *Escherichia coli*

Plasmid DNA was transformed into Top 10 *E. coli* cells utilizing KCM (100 mM KCl, 30 mM $CaCl_2$, and 50 mM $MgCl_2$). Competent cells were thawed on ice then combined with KCM and 1 μg plasmid DNA. The solution was incubated on ice for 15 minutes, incubated at room temperature for 10 minutes, combined with 900 μL LB or TB, and incubated at 37°C with shaking at 220 rpm for 1 hour. Cultures were then spread on LB agar plates with 100 μg/mL ampicillin (LB-AMP) and grown 12-24 hours at 37°C. Single colonies were selected from each transformation and grown 12-24 hours in 6 mL of LB or TB. Five milliliters of this overnight culture were used for plasmid DNA isolation, and 1 mL was used to create a glycerol stock (1:4 culture to 100% glycerol) that was stored in the -80°C freezer.

Transformation of Plasmid DNA into *Saccharomyces cerevisiae*

S1 INsE4A *Saccharomyces cerevisiae* (MATα, ura3-52, leu2-3,112, trp1-289, his7-2, ade5-, 1 lys2::InsE-4[a]) cells were inoculated in 15 mL YPDA broth (1% w/v yeast extract, 2% w/v peptone, 2.5% w/v agar, 0.02% adenine, and 2% w/v glucose), and incubated 12-24 hours at 30°C with shaking. A 1 mL cell pellet was re-suspended in 50% polyethylene glycol, lithium acetate, 10 mg/mL sonicated salmon sperm DNA (Agilent Technologies), 2-mercaptoethanol, and deionized water. The resulting solution was then incubated at 42°C for 15-20 minutes. Cells were then pelleted by centrifugation (2,000 x g) for 2 minutes, and the cell pellet re-suspended in 200 μL deionized water. The re-suspended cells were then spread on selective media plates (0.14% w/v yeast synthetic drop out media, 0.67% w/v yeast nitrogen base, 2.5% w/v agar, 0.002% w/v histidine, 0.005% w/v tryptophan, 0.01% w/v leucine if needed, and 2% w/v glucose) and incubated 24-72 hours at 30°C. Single colonies were selected and streaked on individual (i.e., patch) plates and grown at 30°C for 24 hours.

Yeast Expression

Cells collected from fresh patch plates were inoculated in 15 mL selective media (0.14% w/v yeast synthetic drop out media, 0.67% w/v yeast nitrogen base, 0.002% w/v histidine, 0.005% w/v tryptophan, 0.01% w/v leucine if needed, and 2% w/v glucose) and grown 12-24 hours at 30°C with shaking. OD_{600} values were determined for each culture using a SmartSpec 2000 or SmartSpec Plus spectrophotometer from Bio-Rad (Hercules, CA). Culture volumes needed to make a 0.2 OD_{600} in expression media were

removed from the overnight cultures and centrifuged 1,500 x g for 5 minutes at 4°C. Cells were washed in either deionized water or expression media (0.14% w/v yeast synthetic drop out media, 0.67% w/v yeast nitrogen base, 0.002% w/v histidine, 0.005% w/v tryptophan, 0.01% w/v leucine if needed, 0.5M NaCl if needed, and 2% w/v galactose) depending on application, centrifuged 1,500 x g for 5 minutes at 4°C, then re-suspended in full volume of expression culture (1 mL-100 mL). Expression cultures were grown from 8-60 hours based on application with 6-8 hours resulting in peak ENaC expression. In certain applications OD_{600} readings would be taken at this stage as well. Expression cultures were centrifuged in pre-weighed tubes at 1,500 x g for 5 minutes at 4°C and supernatant was discarded. The cell pellets were stored in -80°C until further use.

pYES2-NTA Expression Vector

Wild type αENaC was cloned into the vector pYES2-NTA from Invitrogen (Carlsbad, CA) by Raquel Ybanez. The vector contains many features that enable expression and detection of αENaC in *S. cerevisiae.* The *GAL1* promoter was used to regulate ENaC expression. In the presence of glucose ENaC expression was repressed, while in the presence of galactose expression was induced. The vector also contains the gene for ampicillin resistance in bacteria used as a selectable marker in bacterial transformation. The *URA3* gene was utilized as a selectable marker in yeast strains lacking *URA3* by allowing cell growth on media lacking uracil to signify successful transformation of the vector into yeast. The presence of the Xpress epitope allowed for protein detection with Western blotting.

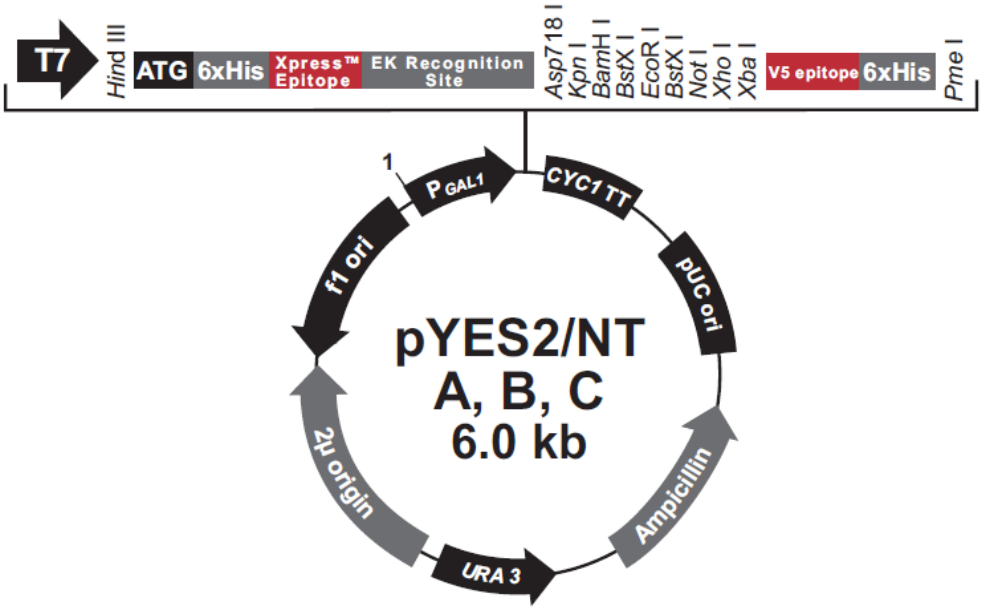

Figure 7: pYES2-NT Expression Vector Map. The alpha ENaC subunit was cloned into the pYES2-NT vector regulated by the GAL1 promoter. This map shows the locations of the regions of functionality of the vector utilized in this investigation.

pESC-LEU Expression Vector

Esther Lee previously cloned both beta and gamma ENaC subunits into the pESC-LEU vector. This vector shares common features with the pYES2-NTA vector including the 2µ and p UC origins of replication and the selective marker for ampicillin resistance. The *LEU2* ORF is used as a selective marker for knock out yeast allowing yeast cells that have successfully transformed the vector to grow on media lacking leucine. This vector contains two multiple cloning sites directly following *GAL* promoters which allowed for two different gene inserts to be cloned into the vector and expressed simultaneously. The multiple cloning site 1 region contains a FLAG epitope while the multiple cloning site 2 region contains a myc epitope. Both epitopes are

immunoreactive and could be utilized for detection of expression products through western blotting.

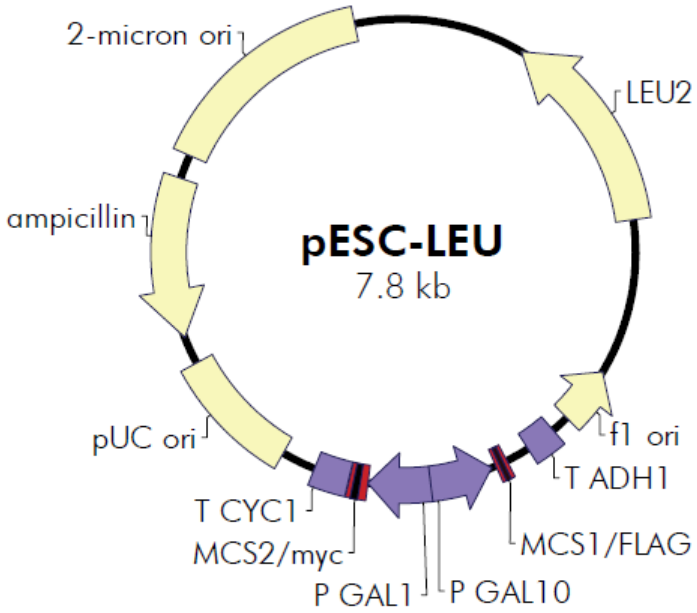

Figure 8: pESC-LEU Expression Vector Map. The gamma ENaC subunit was previously cloned into theMCS1/FLAG site regulated by the GAL10 promoter, and the beta ENaC subunit was cloned into the MCS2/myc site regulated by the GAL1 promoter by Esther Lee. This map shows the locations of the regions of functionality of the vector utilized in this investigation.

Serial Dilution Survival Assay "Pronging"

A dilute stock of yeast cells was created by resuspending cells harvested from fresh patch plates in 500 µL of deionized water. An aliquot of the cells was then diluted 1/40, mixed by vortexing, and sonicated at 3 amps for 8-10 seconds to separate aggregated cells. Cells were counted in each aliquot by adding 12 µL of the dilution to a hemocytometer under a 20X objective lens on an Olympus CKX41 microscope. The average number of cells for each aliquot was used to calculate the number of cells per microliter in each sample. The amount of each stock needed to obtain $1x10^7$ cells in 220

μL of water for each sample was calculated and added to the wells in the first column of a 96 well plate. A five-fold serial dilution was created across six columns of the plate. Diluted cells were pronged onto selective media plates (0.14% w/v yeast synthetic drop out media, 0.67% w/v yeast nitrogen base, 3.0% w/v agar, 0.002% w/v histidine, 0.005% w/v tryptophan, and 0.01% w/v leucine if needed) containing either 2% w/v glucose, 2% w/v glucose with 0.5 M NaCl, 2% w/v galactose, or 2% w/v galactose with 0.5 M NaCl using a pinning tool. The 3% agar plates are important for this assay as they prevent the pinning tool from puncturing the agar. Glucose plates were used to represent cell survival rates with repressed ENaC expression in the presence and absence of added sodium. Galactose plates were used to represent cell survival rate with ENaC expression in the presence and absence of added sodium.

Gene Sequencing and Sequence Analysis

Primers needed for sequencing were identified using the wild type αENaC nucleotide sequence and either selected from current custom primer stocks in the Booth lab, provided by Quintara Biosciences (Berkeley, CA), or designed and ordered from Integrated DNA Technologies, Inc. (Coralville, IA). Quintara Biosciences requires a combination of 10 μl of 80 ng/μl template DNA combined with 5 μl of 5 μM primer to be sent for sequencing for plasmids ≤ 10kb. Personal primer stocks (10 μM) were made by diluting 100 μM freezer stocks from Integrated DNA Technologies (Coralville, IA) 1:10 with sterile water and stored at -20°C until use. Template DNA was prepared by using the concentration of plasmid DNA to be sequenced to calculate the volume needed for an 80 ng/μL sample. Template DNA and primer amounts calculated were combined

with deionized water to create 15 µL samples to be shipped overnight. Sequence data was returned within 24-48 hours.

Table 1: Sequencing Primers

Primer	Sequence
mAlpha ENaC Internal 3	5'-GCAAGGACTGGGCAAGGGGG-3'
Internal ENaC Alpha	5'-GCGAGTGTAGGAAGAGTT-3'
Alpha Internal	5'-ACAACTCTTCCTACACTCGC-3'
CYC1	5'-GCGTGAATGTAAGCGTGAC3'

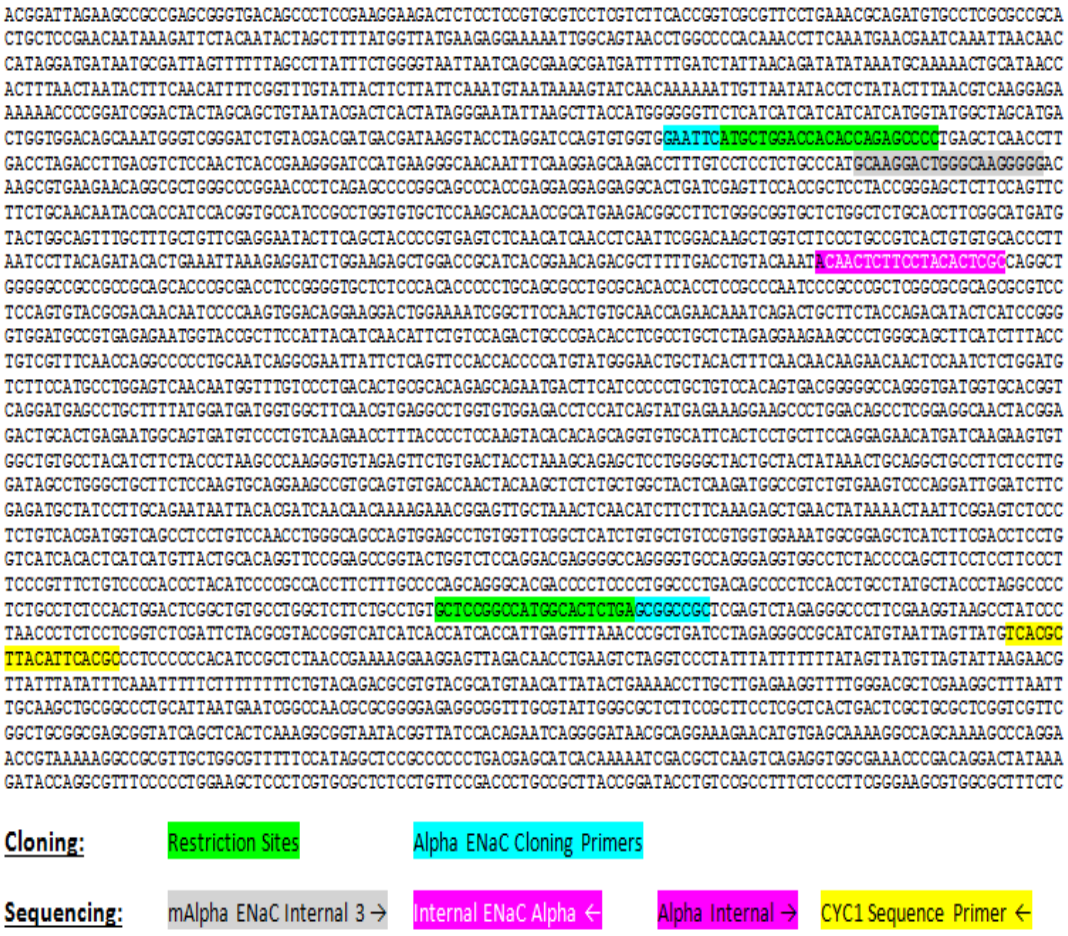

Figure 9: Position of Sequencing Primers in pYES2-NTA/αENaC. An abbreviated sequence of Alpha ENaC/pYES2-NTA, containing the full gene and abbreviated vector sequences, identifies the position and direction of each primer used for sequencing the Alpha ENaC gene.

Sequenced DNA was translated into protein sequences using ExPASy translate tool. These sequences were then aligned with wild type alpha ENaC protein sequence using Clustal Omega. Amino acid changes were identified. Mutations causing amino acid changes were then identified by entering mutated nucleotide sequences into BLAST which aligned with wild type alpha ENaC.

Protein Extractions

Post Alkaline:

Yeast cell pellets were re-suspended in 100 µL of deionized water for every 15-20 mg of wet cell weight. An equal volume of 0.2 M sodium hydroxide added to cell pellets. The cell suspension was incubated for 5 minutes at room temperature then pelleted at 3,000 x g for 5 minutes. Cells were re-suspended in 100 µL of 10X SDS sample buffer (2% v/v SDS, 0.06 M Tris-HCl, 5% v/v glycerol, 4% v/v 2-mercaptoethanol, 0.0025% w/v bromophenol blue) and incubated at 95°C for 5 minutes. Samples were centrifuged at 10,000 x g for 10 minutes and the supernatant was transferred to a new sterile tube without disturbing the cell pellet. This solution was loaded into SDS PAGE gel wells in equal volumes (6-10 µL).

Acid Washed Glass Bead:

A lysis buffer was prepared by adding protease inhibitors (PMSF and EDTA-free cOmplete Mini protease inhibitor cocktail tablet) to RIPA buffer (10 mM sodium

phosphate, 150 mM NaCl, 1% deoxycholate, 1% v/v Triton X-100, 1% w/v SDS at pH 7.2) which was placed on ice until needed. Cell pellets were re-suspended in 100 µL lysis buffer for every 10 mL of expression media. An equal volume of 425-600 µm acid-washed glass beads (Sigma Life Science) were added to each sample and then placed on ice. Samples were vortexed at 2,500 rpm for 30 seconds then placed on ice for 30 seconds alternating for 8 minutes total so each sample had 4 minutes of vortexing. Samples were centrifuged at 10,000 x g for 10 minutes at 4°C and the supernatant was transferred to a microcentrifuge tube without disturbing cell pellet or glass beads. Lysates were quantitated using BCA assay to quantify total protein concentrations, or stored at -80°C until further use.

Mammalian Cell:

Transfected cells were grown in 100 mm Petri dishes by Dr. Boiko at the University of Texas Health and Science Center in San Antonio TX. Once grown to confluence the growth media was removed. Cells were rinsed twice with 5 mL of PBS. A lysis buffer was prepared by adding protease inhibitors (PMSF and EDTA-free cOmplete Mini protease inhibitor cocktail tablet) to RIPA buffer (10 mM sodium phosphate pH 7.2, 150 mM NaCl, 1% w/v deoxycholate, 1% v/v Triton X-100, 1% w/v SDS) and 250 µL was added to each Petri dish. A cell scraper was used to dislodge cells from the bottom of the dish. The resulting solution was incubated overnight at 4°C. Samples were centrifuged at 2,050 x g for 5 minutes to pellet cell debris. The supernatant was transferred to a new microcentrifuge tube and stored at -20°C until further use.

BCA Protein Assay

A BCA assay was performed in a 96 well plate. Twenty-five microliters of deionized water were added to each well position A1-8 and B1-8. Twenty-five microliters of 2 mg/mL BSA (Thermo Scientific) was added to wells A1 and B1 and a 2 fold serial dilution was performed in wells 1-8. A 1/10 dilution was used for each sample to be tested. Twenty-five microliters of each diluted sample was analyzed in duplicate. Two hundred microliters of 50:1 BCA reagents from the BCA Protein Assay Kit (Pierce) were added to each well (standard dilution and protein samples) and quickly mixed. Plate was incubated at room temperature for 5 minutes then incubated at 37°C for 30 minutes. The absorbance at 562 nm was collected in an iMark Microplate Reader (Bio-Rad). A standard curve of BSA concentration vs. absorbance at 562 nm was generated in Microsoft Excel. The equation of the line was used along with absorbance values for each diluted sample to calculate the total protein concentration for each lysate. Cell lysates were then prepared for polyacrylamide gels by adding 100 μg total protein, 1X NuPAGE LDS sample buffer (Invitrogen), and 2.5% v/v 2-mercaptoethanol. Samples were incubated at 95°C for 5 minutes before loading into a polyacrylamide gel.

Sodium Dodecyl Sulfate Polyacrylamide Gel Electrophoreses (SDS PAGE)

SDS PAGE gels were made with 4% stacking gel (7.5% acrylamide, 0.1% w/v SDS, 0.1 % w/v ammonium persulfate, 0.375 M Tris-HCl, pH 8.8, 0.08% TEMED) and 7.5% resolving gel (4% acrylamide, 0.1% w/v SDS, 0.05% w/v ammonium persulfate, 0.125 M Tris-HCl pH 6.8, 0.1% TEMED) using 1.5 mm casters (Bio-Rad). Resolving

gel was added to cast first, topped with ethanol, and allowed to solidify 30 minutes. Ethanol was poured off and allowed to dry completely. Stacking gel was filled to top of the cast before adding the well comb and then left to solidify 45 minutes. Gels that were not used right away were stored in running buffer (25 mM Tris-HCl, 200 mM glycine, and 0.1% w/v SDS, pH 8) at 4°C until use. Gels were then added to vertical gel rig, PageRuler Plus pre-stained ladder was used as a standard in one well, samples were loaded into remaining gel wells, and separation by electrophoresis was conducted at 100 V for 70 minutes.

Transferring Protein to Nitrocellulose Blot

Proteins from SDS PAGE gels were transferred to nitrocellulose blotting material using Trans-Blot Turbo™ RTA Transfer Kit and Trans-Blot Turbo™ Transfer System (Bio-Rad). Two transfer stacks and one nitrocellulose membrane were used per gel and were prepped by equilibrating in 1X Trans-Blot® Turbo™ Transfer Buffer (20% 5X Transfer Buffer, 60% nanopure water, and 20% v/v ethanol) for 2-3 minutes. The first transfer stack was placed on the bottom of the cassette followed by the nitrocellulose, SDS PAGE gel, and then last transfer stack. The top of the cassette was securely fastened and the cassette was placed in the transfer system and run at 20V, 1.3 constant amps, for 20 minutes. Transfer stacks and SDS PAGE gels were disposed of in an appropriate liquid waste container and the blot was ready for downstream applications.

Western Blot

The nitrocellulose membrane was incubated in 5 mL of blocking solution (5% w/v non-fat dry milk in TBST (1X Tris-buffered saline, and 0.1% v/v Tween)) and agitated on a rocker for 30 minutes. Blocking solution was discarded and the blot was washed in 20 mL TBST for 5 minutes on a rocker. Primary antibody was added in concentration specified for particular antibody being used and incubated 12-16 hours at 4°C with gentle rocking. The antibody dilution was removed and stored at 4°C for re-use. The blot was washed three times with TBST for five minutes each. Secondary antibody was added in concentration of 1/20,000 and agitated on the rocker for 1 hour. The blot was rinsed three times in TBST for five minutes each with a final rinse in 20 ml 1X TBS for 5 minutes. Western Lightning® Plus-ECL (Perkin Elmer) reagents were mixed (750 µL each reagent) in low light conditions and added directly and evenly to blot and allowed to bind in the dark for at least one minute. Solution was removed from blot and a long exposure image was collected using ChemiDoc XRS+ Imaging System running Image Lab 5.1 software by Bio-Rad (Hercules, CA). Five total images were taken in succession; one image every minute, for 5 minutes. A custom image setting allowed an image of the blot with the ladder to be collected. The software allows merging of these images to allow visualization of protein bands and standard ladder together.

Antibody Stripping

Blots were stripped by adding 20 mL stripping solution (62.5 mM Tris-HCl, pH 8, 2% w/v SDS, and 0.7% v/v 2-mercaptoethanol) and incubating at 55°C with rocking for 12 minutes. The blots were then rinsed for 1-2 hours with deionized water changing the water every 30 minutes. The blots were rinsed with 20 mL of TBST for 15 minutes, and then blocked in 5% w/v blocking solution (5% w/v non-fat dry milk in TBST). Blots were rinsed 5 minutes in TBST and new primary antibody was applied and incubated overnight with rocking.

Time Course Growth Assay

Cells collected from fresh patch plates were inoculated in 15 mL 2% glu-ura selective media and grown 24 hours at 30°C with shaking. Samples were pulled from the incubator and OD_{600} values were determined using a SmartSpec 2000 or SmartSpec Plus spectrophotometer from Bio-Rad (Hercules, CA). These values were used to inoculate 100 mL expression cultures to a starting OD_{600} of 0.2. The culture aliquots were centrifuged 1,500 x g for 5 minutes at 4°C. Cells were washed in 2% gal-ura + 0.5 M NaCl expression media, centrifuged 1,500 x g for 5 minutes at 4°C, re-suspended in 100 mL of expression media, and the initial OD_{600} absorbances were immediately measured. Expression cultures were then placed in 360 Orbital Shaker Bath (Precision Scientific) at 30°C at approximately 200 rpm. Aliquots (500 µL) were taken every 3 hours and OD_{600} absorbances measured until cultures completed a cycle through lag, log, and stationary phase. Aliquots were taken for up to 60 hours. as needed without incurring over 10%

loss in culture volume. Absorbances for each time period were used to create a graph in Microsoft Excel and growth rates were compared using the slope of the best fit line for each sample.

Cloning

Restriction Digest:

Digestion of βENaC in pCMV-MYC and alpha random mutant ENaCs in pYES2-NTA were completed in reactions containing approximately 1.0 µg plasmid DNA, 1X CutSmart Buffer (New England Biolabs), 10 units of EcoRI-HF (New England Biolabs), 10 units of NotI-HF (New England Biolabs), in a total reaction volume of 25 µL. Reactions were incubated at 37°C for two hours and stopped using 1X EndorStop sample buffer. Restriction products were then analyzed by horizontal gel electrophoresis in a 0.7% w/v TAE agarose gel run at 85 V for 90 minutes.

Gel Extraction and Purification:

Restriction products in agarose gels were visualized using a Foto/Phoresis UV Transilluminator from Fotodyne Inc. (Hartland, WI). DNA fragments were then extracted and cleaned using Qiagen QIAquick Gel Extraction Kit (Valencia, CA) following the manufacturer's protocol.

Ligation:

Ligation of the mutant ENaC genes with the pCMV-MYC vector was accomplished by setting up reactions with a 3:1 insert to vector ratio. These reactions contained 3:1 ratio insert to vector volumes, 1X T4 DNA Ligase Buffer (New England Biolabs), 400U T4 DNA ligase (New England Biolabs), and sterile water to bring to a volume of approximately 20 µL. DNA insert masses required for these reactions were generated using New England Biolabs Ligation Calculator tool. Reactions were incubated at room temperature for 10 minutes, then heat inactivated at 65°C for 10 minutes. The ligated solution was then transformed in 5 µL aliquots into Top 10 *E. coli* cells utilizing standard KCM protocol with incubation in 6 mL Terrific Broth. Transformation reactions were plated on LB-AMP (100 µg/mL) plates and grown overnight at 37°C. Single colonies were selected from transformation plates and grown overnight in TB-AMP then subjected to the plasmid isolation protocol.

Ligation Confirmation with Restriction Digest:

Ligated plasmid DNA was subjected to a double restriction digest to confirm correct ligation. Approximately 2 µL plasmid DNA were combined with 20 U BamHI (New England Biolabs) and 1X NEBuffer 3.1 in a reaction volume of approximately 25 µL. Samples were incubated at 37°C for 2 hours, and analyzed by horizontal gel electrophoresis in a 50 mL 1.5% w/v TAE agarose gel at 100 V for 75 minutes.

III. RESULTS AND DISCUSSION

The goal of this project was to identify residues within the extracellular loop of the alpha subunit of the epithelial sodium channel that are critical for proper function. Preliminary studies in the Booth lab utilized error prone PCR to induce random mutations within the gene corresponding to the extracellular loop domain of the alpha ENaC subunit and screened for homomeric channel function. The current project further screened and characterized the function of these mutants compared to wild type αENaC. Eleven mutants (101, 108, 117, 118, 123, 124, 129, 130, 132, 134, and 138) were utilized for further characterization in homomeric and heteromeric channel studies.

Mutant αENaC Screening in Yeast

Eleven mutants of interest were chosen from preliminary screenings previously conducted in the Booth lab. Mutants were chosen by analyzing previous serial dilution assays and selecting mutations that showed changes in cell survival when compared to wild type. pYES2-NTA/αENaC 117, 130, and 134 were stored by previous students as isolated plasmid at -80°C. These mutants were transformed into Top 10 *E. coli* cell utilizing the high efficiency KCM protocol and grown 24 hours on LB-AMP plates. The remaining mutants (101, 108, 118, 123, 124, 129, 132, and 138) had been previously stored in Top 10 *E. coli* glycerol stocks at -80°C. Samples of each *E. coli* mutant were grown overnight in 5 mL LB-AMP broth. Plasmid DNA was isolated using the Qiagen QIAprep Spin Miniprep kit (Valencia, CA) following the manufacturer's protocol. Concentrations of each sample were determined using the NanoDrop 2000

Spectrophotometer from Thermo Scientific (Waltham, MA) and stored at -20°C until further use. Each mutant plasmid was then transformed into S1INsE4A *S. cerevisiae* for use in functional studies.

Homomeric Channel Serial Dilution Survival Assay "Pronging"

To characterize salt sensitivity and protein function, each αENaC mutant was subjected to a serial dilution pronging assay. This qualitative assay demonstrated ENaC function based on yeast cell growth inhibition (i.e. functional ENaC results in sodium movement into the cell causing growth inhibition). The number of cells present could be correlated to cell survival while the diameter of the growth can be correlated to growth rate. The growth of yeast colonies from each mutant were compared to wild type αENaC as well as yeast cells transformed with empty vector pYES2-NTA. Pronging assays were conducted for 4 independent colonies (n=4) of αENaC in pYES2-NTA (Figures 10 and 11).

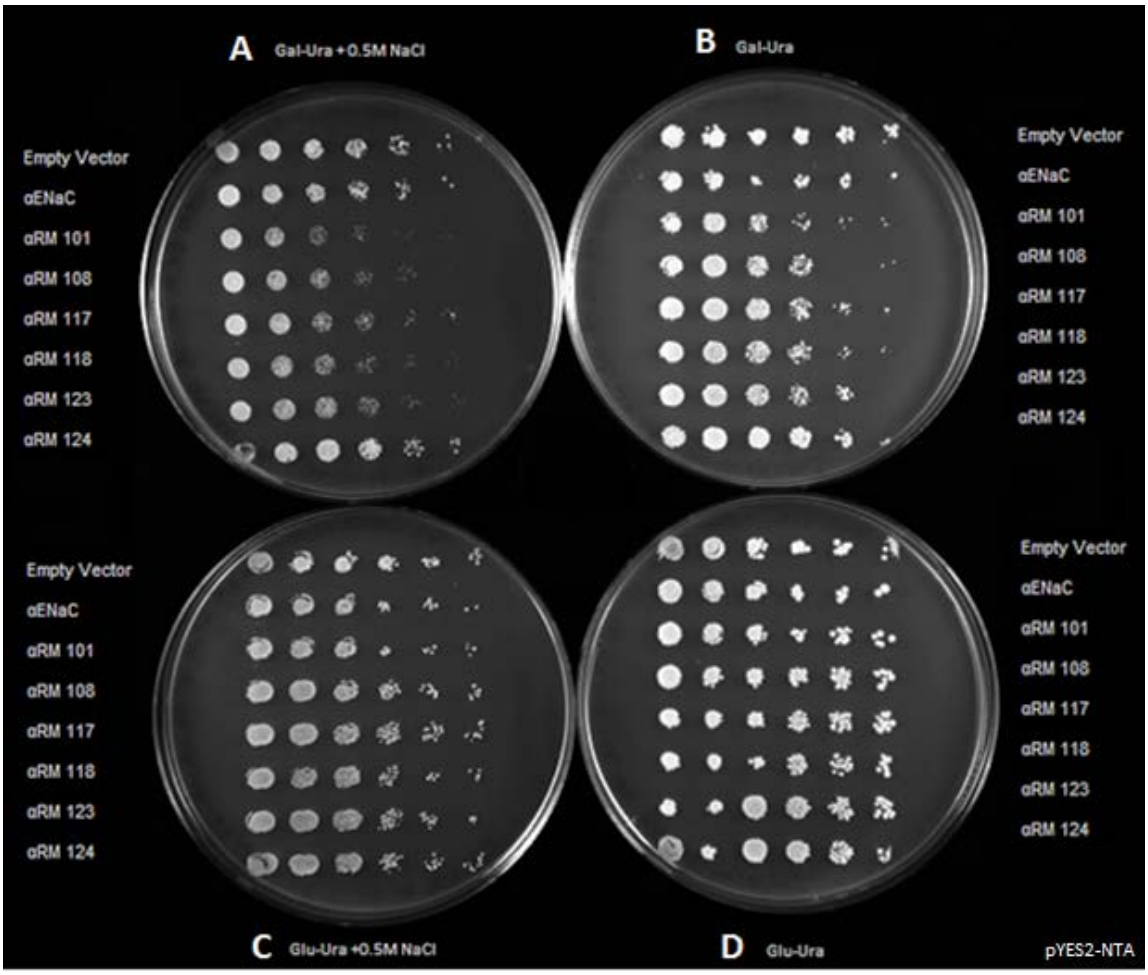

Figure 10: Alpha ENaC Mutants 101-124 Homomeric Pronging Assay. (n=4, 72 hrs.) (A) Effect of expressed ENaC in the presence of additional 0.5 M NaCl. (B) Effect of expressed ENaC in the presence of minimal NaCl. (C) Effect of repression of ENaC in the presence of additional 0.5 M NaCl. (D) Effect of repression of ENaC in the presence of minimal NaCl.

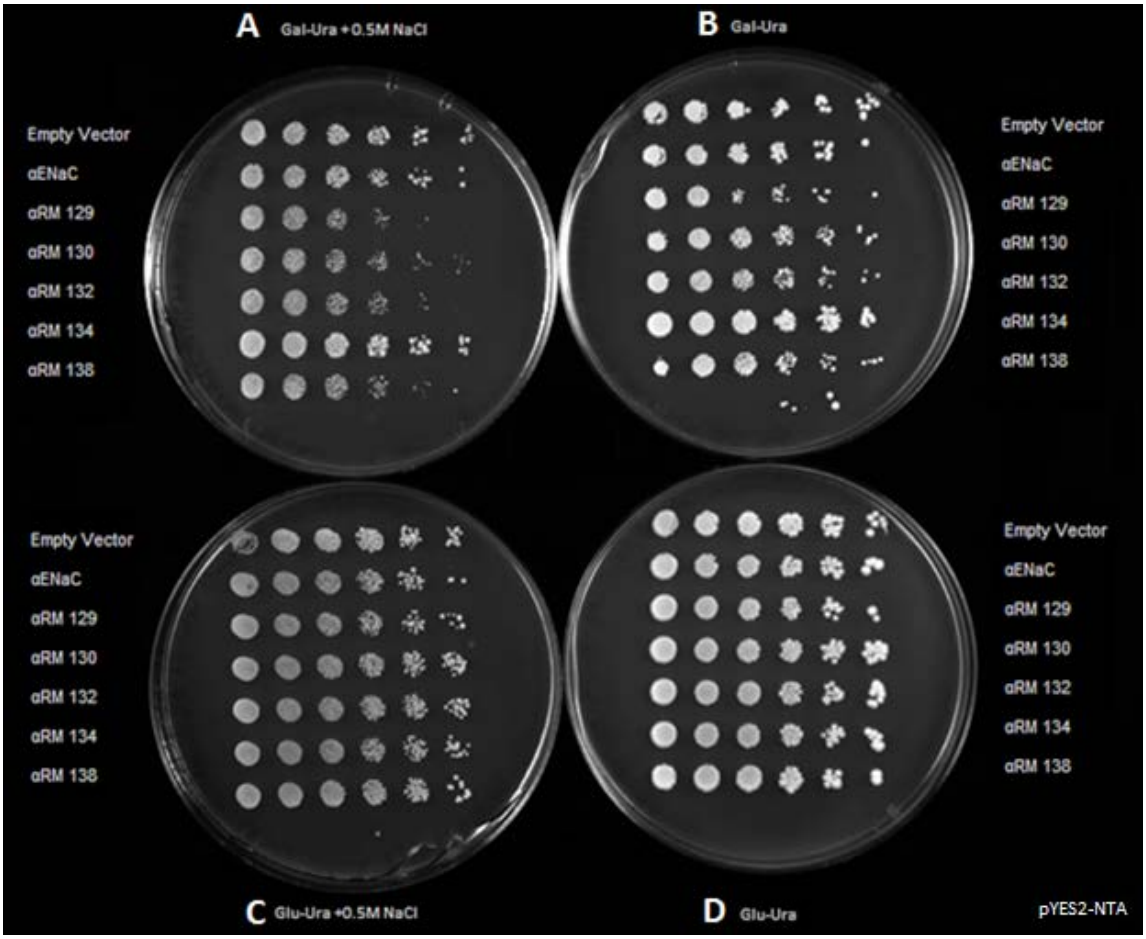

Figure 11: Alpha ENaC Mutants 129-138 Homomeric Pronging Assay. (n=4, 96 hrs.) (A) Effect of expressed ENaC in the presence of additional 0.5 M NaCl. (B) Effect of expressed ENaC in the presence of minimal NaCl. (C) Effect of repression of ENaC in the presence of additional 0.5 M NaCl. (D) Effect of repression of ENaC in the presence of minimal NaCl.

Alpha random mutants (aRM) 117, 123, 129, 130, and 132 displayed decreased cell survival in all trials indicating increased function of ENaC within these cells. These results were consistent with preliminary functional screenings conducted by Chance Berman. They were also consistent between multiple colonies (n=4) pronged from the same transformation. Alpha random mutant 134 shows slightly increased growth, or lack of growth inhibition, suggesting decreased functionality of ENaC. This result was also consistent with previous functional screenings, and between multiple colonies (n=4)

pronged from the same transformation. Alpha random mutants 101, 108, 118, and 138 displayed decreased cell survival which does not support previous findings, but were consistent in functional trend between all colonies (n=4) pronged from this transformation. Alpha random mutant 124 showed slightly increased growth, which does not support previous findings, but was also consistent in functional trend between all colonies (n=4) pronged from this transformation. Due to the consistency seen between multiple colonies, all mutants screened were used in heteromeric functional studies.

Heteromeric Channel Studies

ENaC studies have demonstrated that heteromeric channels generate higher currents than homomeric channels (7), thus αENaC mutant was co-expressed to produce heteromeric channels. Two possible outcomes were expected from heteromeric channel studies in yeast. The first outcome predicted that the function of heteromeric channels would be greater than homomeric αENaC channels with more pronounced change in function due to the addition of beta and gamma subunits as seen in mammalian systems. The second outcome predicted that the beta and gamma subunits lacking mutations could rescue functional changes (gain or loss) caused by the alpha mutation resulting in currents that mimic the wild type channel.

Wild type beta and gamma genes in pESC-LEU were transformed into S1 yeast containing αENaC using the lithium acetate transformation protocol and subjected to functional studies (Figures 15 and 16). Functional studies were also conducted on S1 αENaC yeast cells transformed with empty pESC-LEU vector (Figures 12 and 13) to

show that the vector itself had no effect on ENaC function. Pronging assays were conducted for 3 colonies (n=3) from each transformation plate to test for reproducibility.

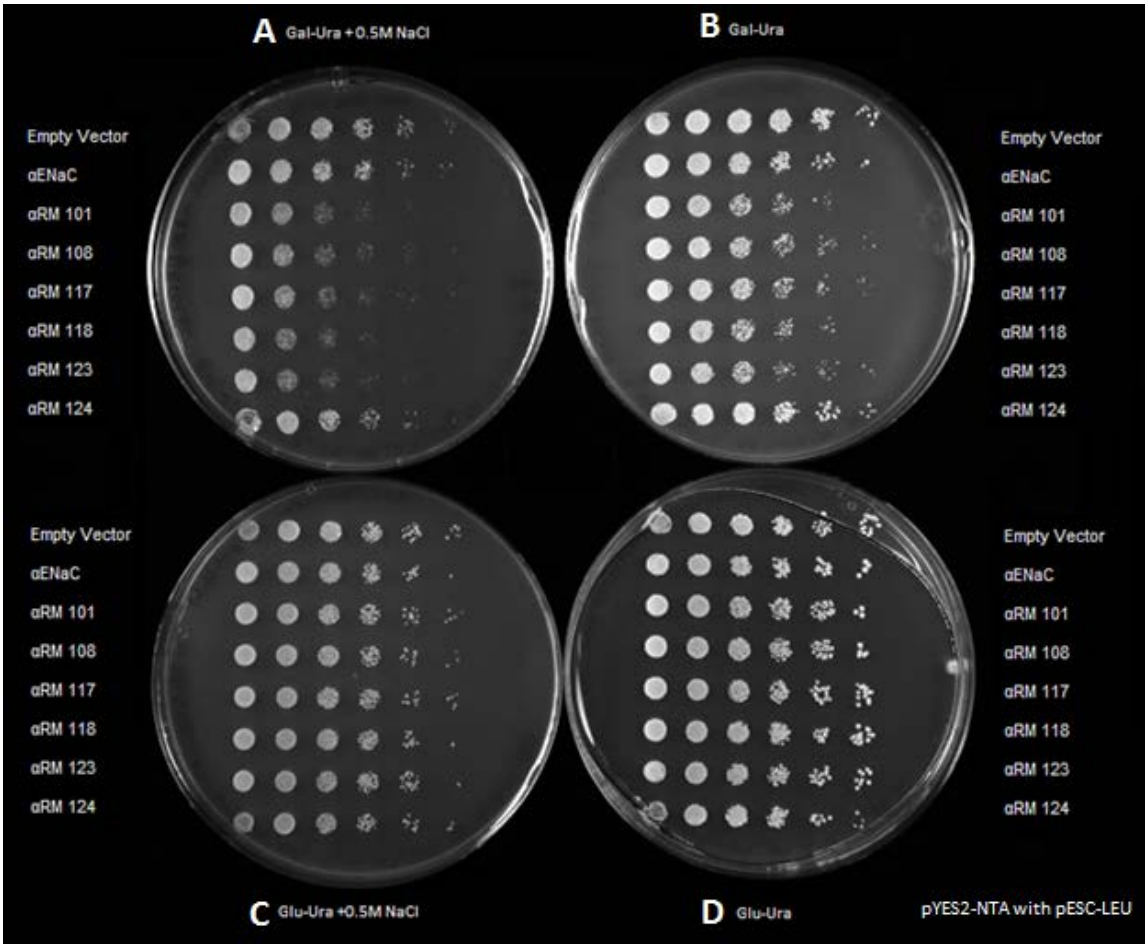

Figure 12: Alpha ENaC Mutants 101-124 pYES2-NTA with pESC-LEU Pronging Assay. (n=3, 72 hrs.) (A) Effect of expressed ENaC with pESC-LEU in the presence of additional 0.5 M NaCl. (B) Effect of expressed ENaC with pESC-LEU in the presence of minimal NaCl. (C) Effect of repression of ENaC with pESC-LEU in the presence of additional 0.5 M NaCl. (D) Effect of repression of ENaC with pESC-LEU in the presence of minimal NaCl.

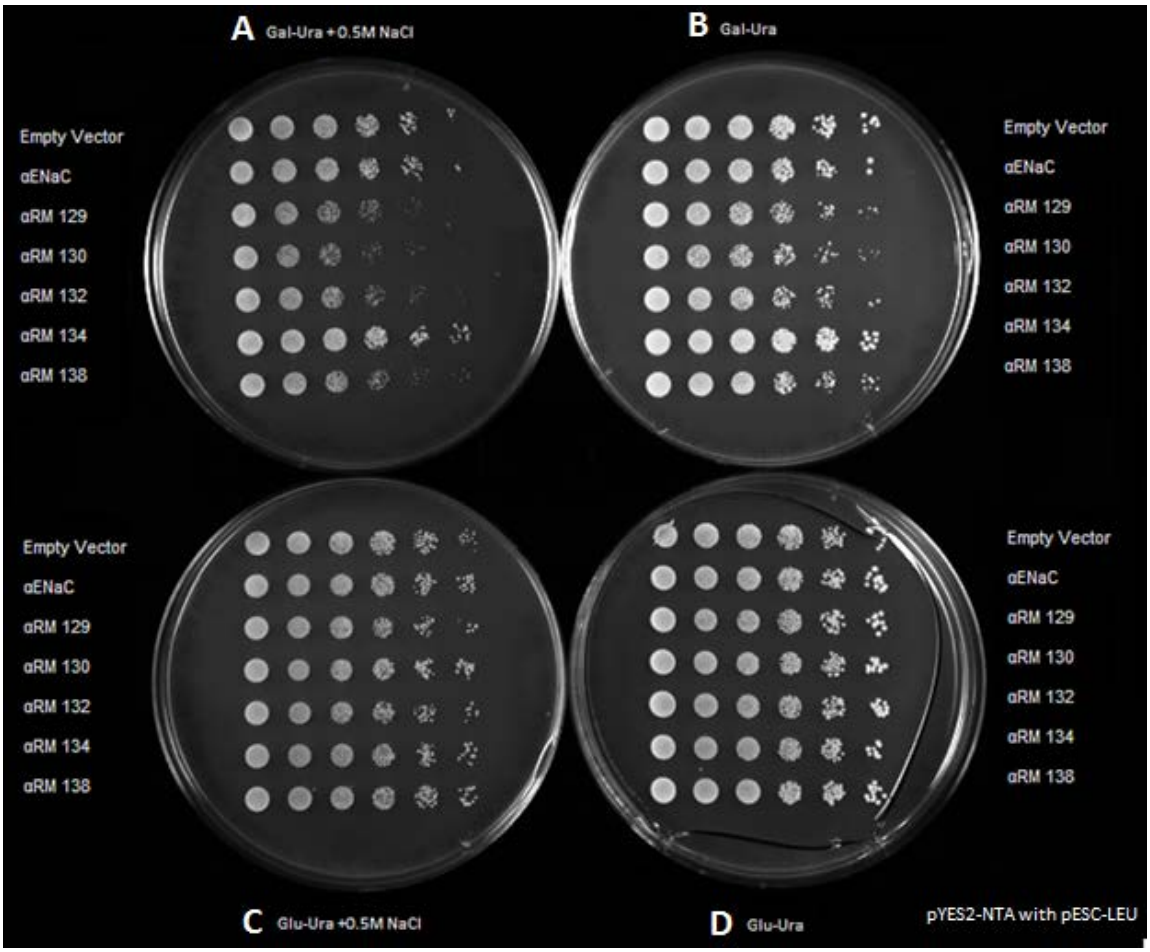

Figure 13: Alpha ENaC Mutants 129-138 pYES2-NTA with pESC-LEU Pronging Assay. (n=3, 96 hrs.)(A) Effect of expressed ENaC with pESC-LEU in the presence of additional 0.5 M NaCl. (B) Effect of expressed ENaC with pESC-LEU in the presence of minimal NaCl. (C) Effect of repression of ENaC with pESC-LEU in the presence of additional 0.5 M NaCl. (D) Effect of repression of ENaC with pESC-LEU in the presence of minimal NaCl.

Alpha random mutants 101, 108, 117, 118, 123, 129, 130, 132, and 138 (Figures 12 and 13) all show decreased survival correlated to an increased functionality of the channel. Alpha random mutants 124 and 134 (Figures 12 and 13) suggest slightly increased growth correlated to a decreased functionality of the channel. These functional trends for each mutant were consistent with results from αENaC homomeric pronging assays showing that the presence of empty pESC-LEU vector has no effect on functionality.

Validation of βγpESC-LEU Plasmid Stock

To verify the pESC-LEU/βγENaC plasmid, sample digestion reactions were completed and analyzed by horizontal gel electrophoresis. ZraI (New England Biolabs) was used to cut the beta gene and BglII (New England Biolabs) was used to cut the gamma gene. Digestion reactions were also carried out for empty pESC-LEU, pESC-LEU/βENaC and pESC-LEU/γENaC as controls. Due to the conditions required for efficient function of BglII and ZraI a double digest was not possible for pESC-LEU/βγENaC and a sequential digest was used. The sequential digest for pESC-LEU/βγENaC was carried out in two reactions. The first reaction was incubated with ZraI at 37°C for 1 hour, and then incubated at 80°C for 20 minutes to heat inactivate the enzyme. Five microliters of 1 M NaCl was added to increase the salt concentration to 100 mM for the second reaction. BglII (1 µL) was added and the second reaction was incubated at 37°C for 1 hour.

Reactions were analyzed with horizontal gel electrophoresis using a 1% w/v TAE agarose gel run at 110 V for 1 hour (Figure 14). The gel was stained with ethidium bromide and restriction products visualized with ultraviolet light on the ChemiDoc XRS+ Imaging System running Image Lab 5.1 software by Bio-Rad (Hercules, CA).

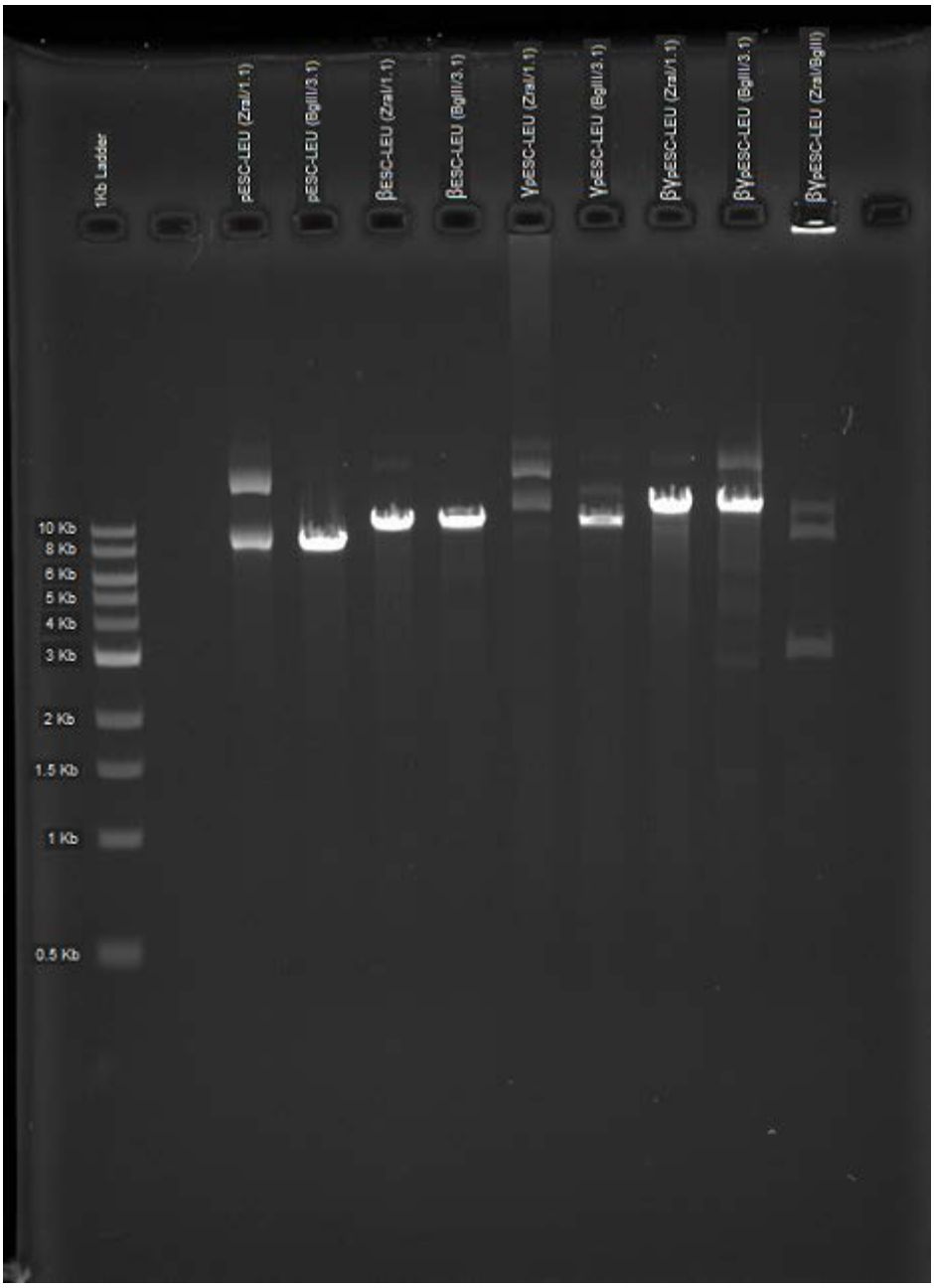

Figure 14: Restriction Digest Reactions for pESC-LEU/βγ ENaC Validation. Empty vector pESC-LEU, βpESC-LEU, and βγpESC-LEU samples were subjected to restriction digestions with ZraI and BglII.

Empty vector pESC-LEU has no restriction site for ZraI so two DNA fragments >10,000 bp and ~9,000 bp were visualized representing nicked open circular and supercoiled forms of the plasmid, respectively. Empty pESC-LEU digested with BglII

produced a band at ~7,800 bp. A single digest of pESC-LEU/βENaC with ZraI or BglII produced a band at ~9,600bp. There was no restriction site for ZraI in pESC-LEU/γENaC so two DNA fragments were visualized, both greater than 10,000 bp, representing circular and supercoiled forms of the plasmid. A single digest of pESC-LEU/γENaC produced a single DNA fragment at ~ 9,600 bp. A single digest of pESC-LEU/βγENaC with ZraI or BglII produced a single DNA fragment at ~11,600 bp. A sequential digest of pESC-LEU/βγENaC resulted in a total of three DNA fragments. The DNA fragment at ~11,600bp corresponds to plasmids that were only partially digested by one of the two enzymes present. The fragments at ~8,500 bp and ~3,000 bp correspond to the lengths of plasmid successfully digested by both enzymes. This gel confirms the presence of both the beta and gamma ENaC genes within the pESC-LEU vector (Figure 14).

Serial Dilution Survival Assay "Pronging" pYES2-NTA/αENaC with pESC-LEU/βγENaC

The second set of pronging assays completed for heteromeric channel studies were those for the αENaC samples transformed with pESC-LEU/βγENaC. These cells are capable of producing mutant αENaC along with wild type βγENaC simultaneously. The growth of yeast colonies from each mutant were compared to αENaC homomeric pronging assays. Heteromeric pronging assays were conducted for three colonies (n=3) from each transformation plate to test for reproducibility.

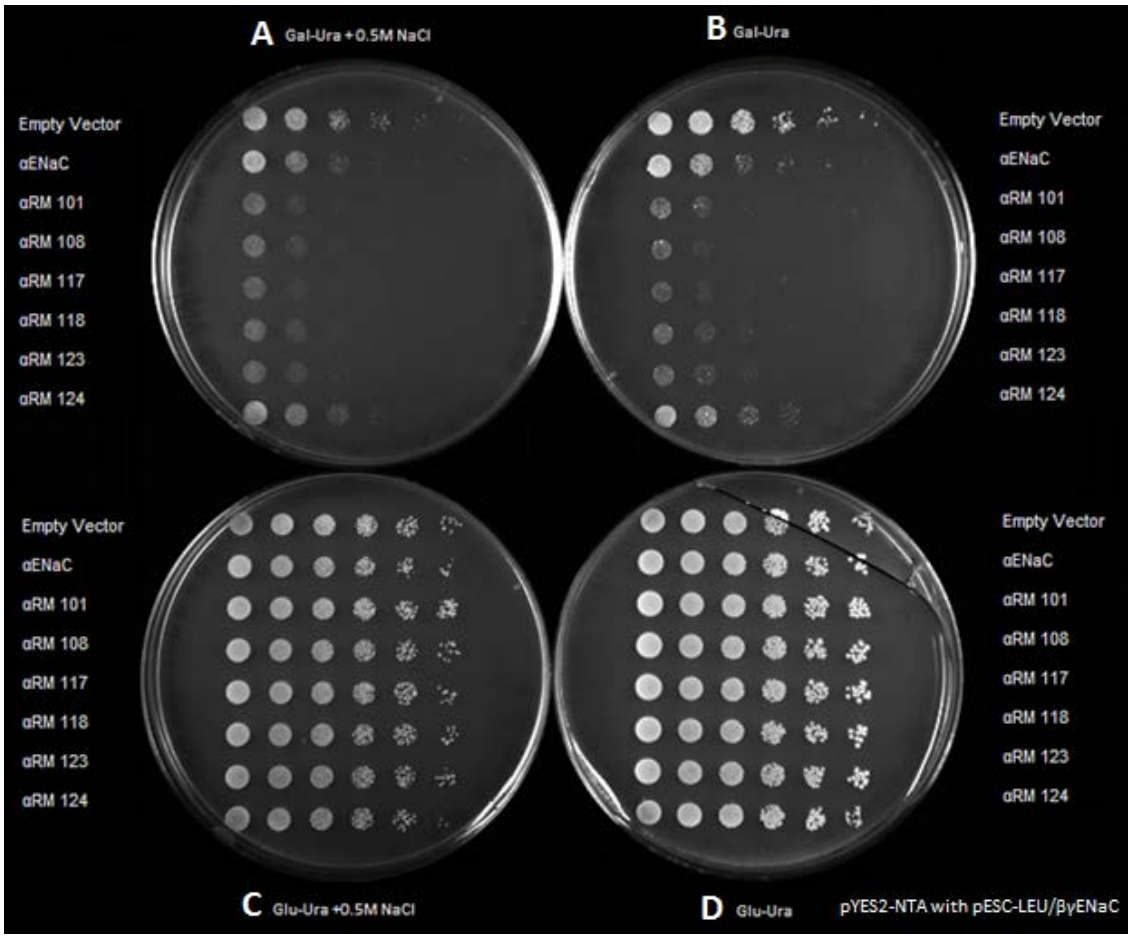

Figure 15: Alpha ENaC Mutants 101-124 pYES2-NTA with pESC-LEU/βγENaC Heteromeric Pronging Assay. (n=3, 96 hrs.)(A) Effect of expressed ENaC with βγpESC-LEU in the presence of additional 0.5 M NaCl. (B) Effect of expressed ENaC with βγpESC-LEU in the presence of minimal NaCl. (C) Effect of repression of ENaC with βγpESC-LEU in the presence of additional 0.5 M NaCl. (D) Effect of repression of ENaC with βγpESC-LEU in the presence of minimal NaCl.

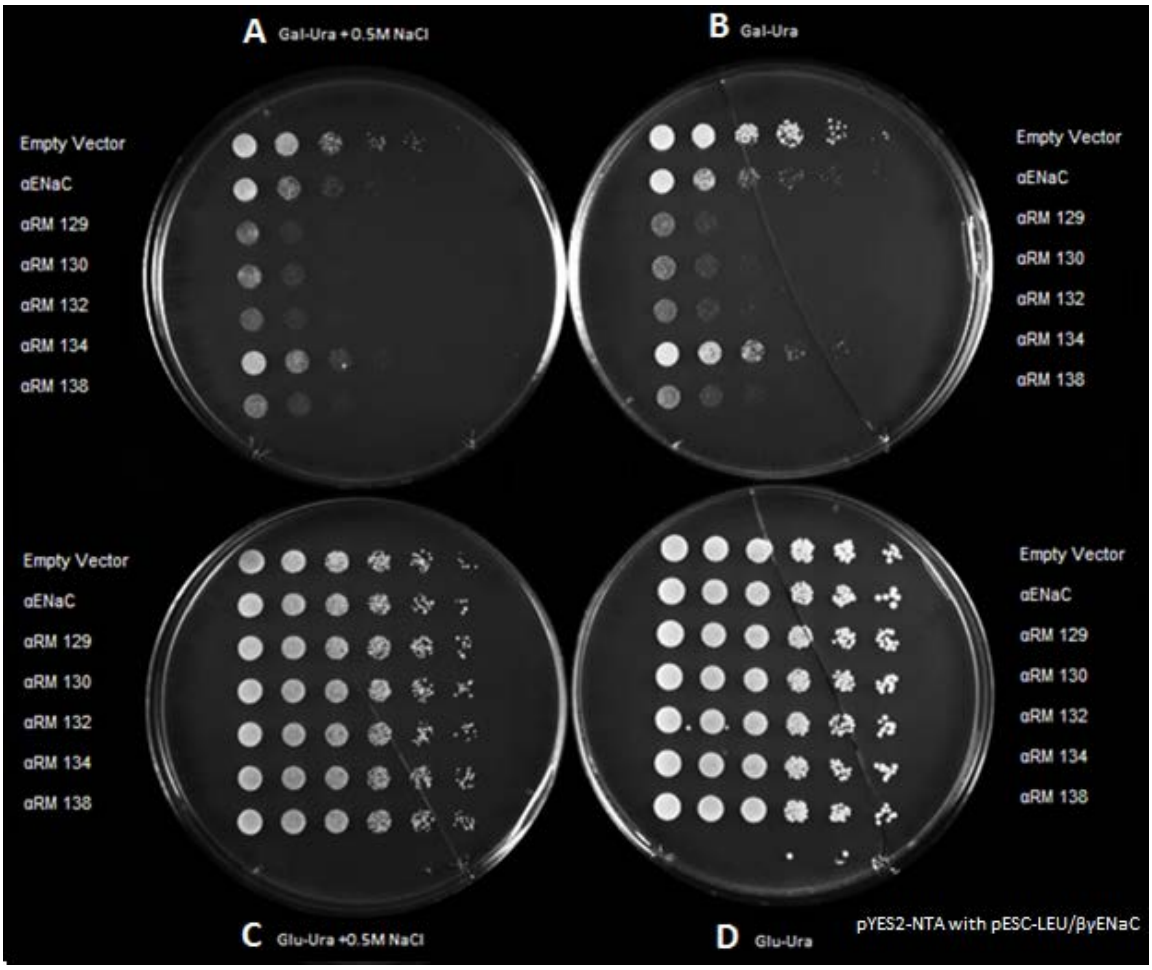

Figure 16: Alpha ENaC Mutants 129-138 pYES2-NTA with pESC-LEU/βγENaC Heteromeric Pronging Assay. (n=3, 96 hrs.)(A) Effect of expressed ENaC with βγpESC-LEU in the presence of additional 0.5 M NaCl. (B) Effect of expressed ENaC with βγpESC-LEU in the presence of minimal NaCl. (C) Effect of repression of ENaC with βγpESC-LEU in the presence of additional 0.5 M NaCl. (D) Effect of repression of ENaC with βγpESC-LEU in the presence of minimal NaCl.

All samples, including wild type, showed an increased sensitivity to salt when compared to homomeric prongings (Figures 10 and 11). The increase in function of the heteromeric channels was strongly suggested in these assays. When compared to wild type alpha random mutants 101, 108, 117, 118, 123, 129, 130, 132, and 138 show decreased cell survival (Figures 15 and 16) which correlated to an increase in function of the channel. Alpha random mutants 124 and 134 showed an increase in cell survival

(Figures 15 and 16) correlating to a decrease in function of the channel. The functional trends for each alpha mutant were consistent with results from wild type and mutant αENaC homomeric pronging assays.

Since the function of each alpha mutant remained consistent in homomeric and heteromeric channel pronging studies the next step of this investigation was to obtain the nucleotide sequences of the mutants for sequence analysis. Each plasmid DNA was sent for nucleotide sequencing and the position of each mutation was identified.

Mutant Sequencing and Protein Alignment

The alpha ENaC gene was sequenced for each mutant using four separate primers: mAlpha ENaC Internal 3, Internal ENaC Alpha, Alpha Internal, and CYC1. Each mutant was sequenced in four reactions, one per primer, by Quintara Biosciences (Berkeley, CA). Mutant nucleotide sequences were translated into protein sequences using the ExPASy translate tool (http://web.expasy.org/translate/). Protein sequences were aligned and compared to wild type *Mus musculus* SCNN1A amino acid sequence using the Clustal Omega multiple sequence alignment tool (http://www.ebi.ac.uk/Tools/msa/clustalo/) to identify changes in the amino acid sequence (Figure 17). Mutants 101, 118, and 129 were the only mutant strains that contained a single amino acid change, and were the only mutants used in further studies.

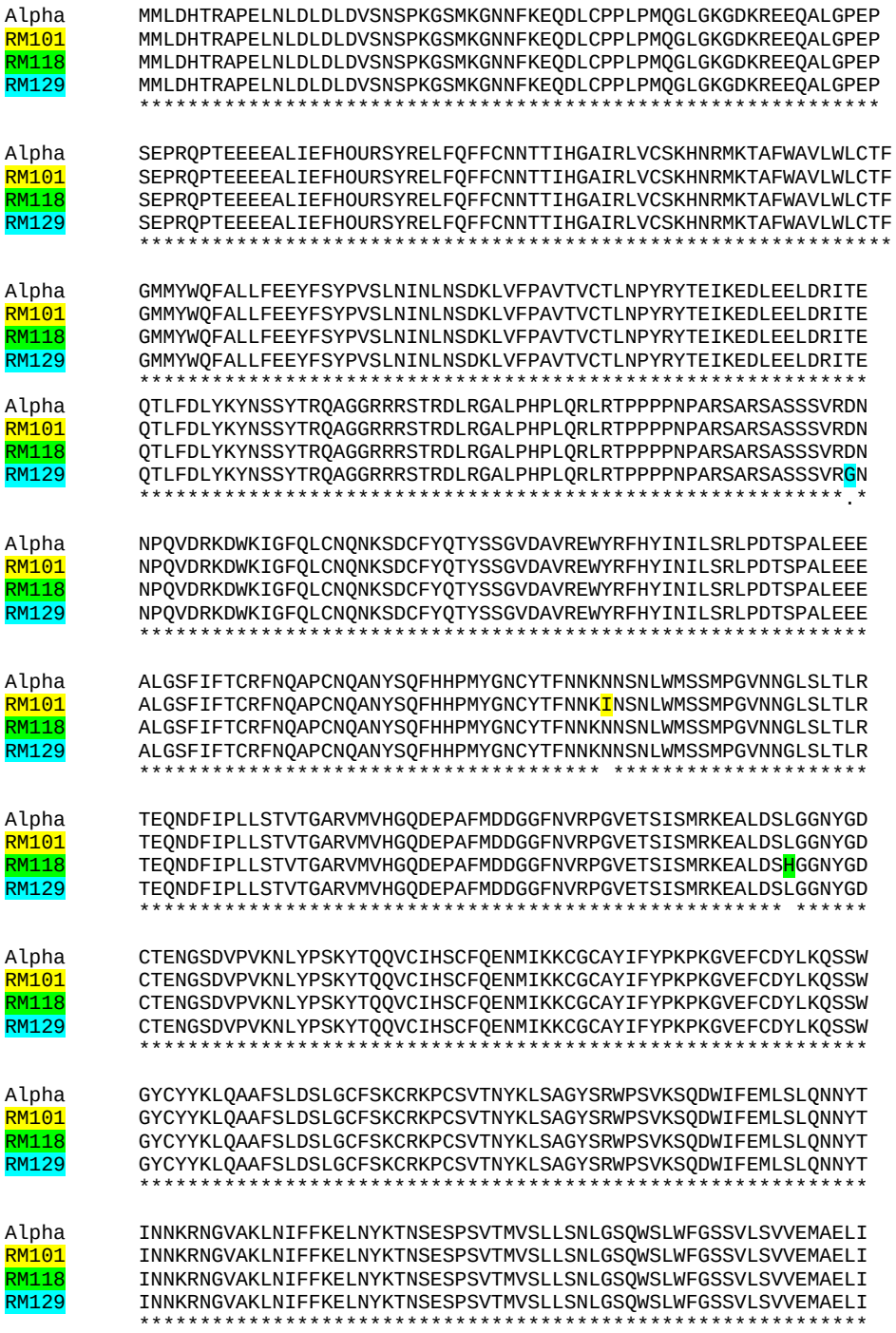

Figure 17: Multiple Protein Sequence Alignment. Protein sequences for aRM101, aRM118, and aRM129 were aligned with wild type Alpha ENaC protein sequence. The asterisk beneath each position signifies identity between sequences. Amino acid changes are highlighted in colors corresponding to the sample they are contained within. Alignment was generated using Clustal Omega.

Alpha random mutant 101 contains a change from a polar amino acid, asparagine, to a non-polar amino acid, isoleucine, at position 339 (N339I). Alpha random mutant 118 contains a change from a non-polar amino acid, leucine, to a positively charged basic amino acid, histidine, at position 414 (L414H). Alpha random mutant 129 contains a change from a negatively charged acidic amino acid, aspartate, to a non-polar amino acid, glycine, at position 239 (D239G).

Each mutation is characterized by an amino acid substitution which changes the chemical property of the residue. Charged and polar amino acids are electrostatically attracted to other polar and charged molecules. If a charged or polar amino acid were substituted for a non-polar amino acid, it would result in a conformational change in the three-dimensional structure of the protein at that point. This would be caused due to repulsion of this non-polar residue from the surrounding charged or polar residues it previously interacted with. The same would be true for a non-polar amino acid being substituted for a charged or polar amino acid. The change in chemical property of these mutations may be the cause of the increased ENaC function observed in yeast screens.

Nucleotide Sequence Alignment

Once mutants were identified to contain only a single amino acid change, the section of the nucleotide sequence causing the amino acid change was identified. All amino acid changes were contained within the protein sequences translated from the sequences obtained from the Alpha Internal primer. This section of the nucleotide sequence for each mutant was individually aligned with the wild type *Mus musculus* SCNN1A nucleotide sequence to identify point mutations using nucleotide BLAST

software. All mutant sequences were then aligned with wild type using Clustal Omega software (Figure 18).

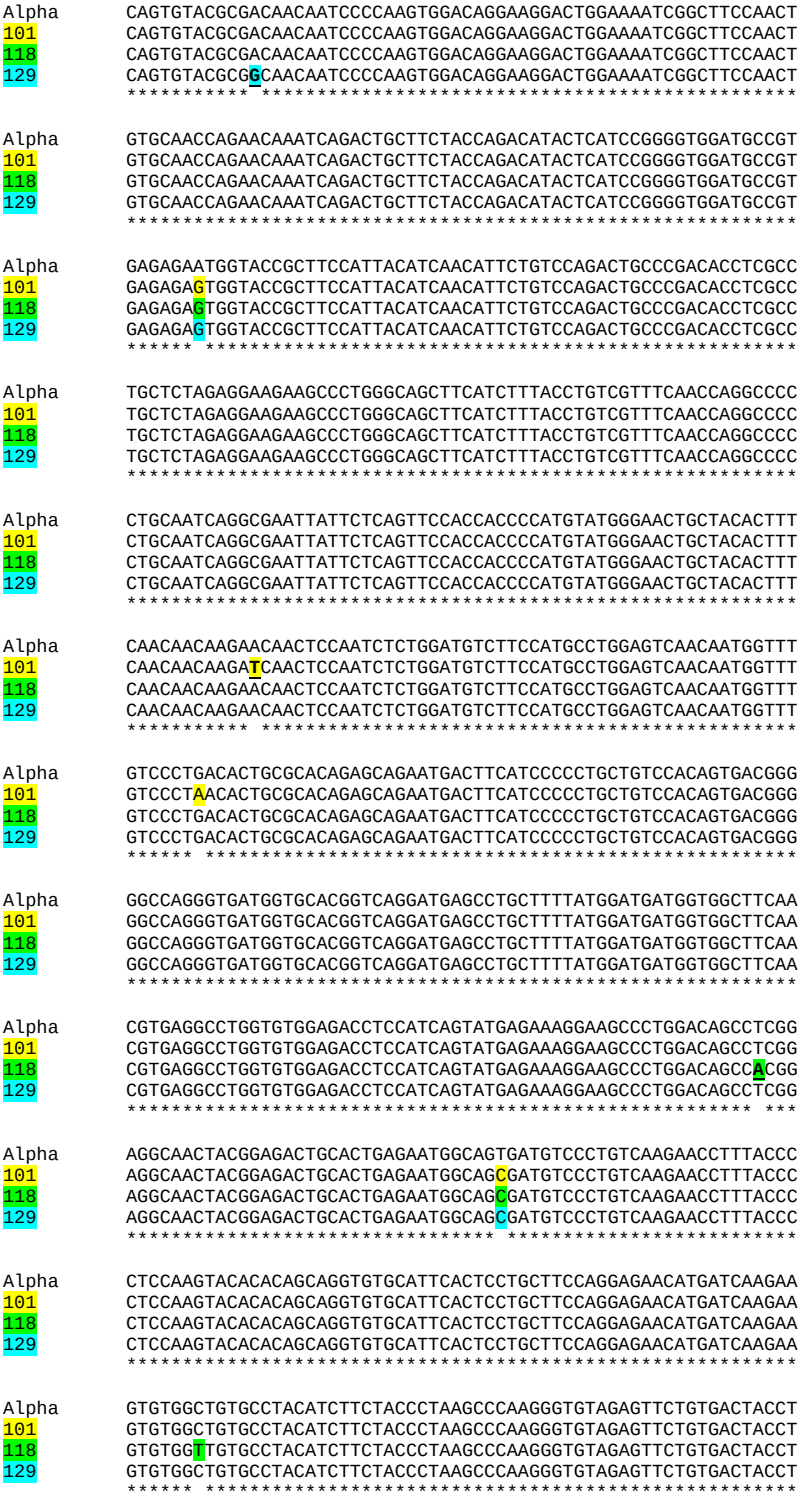

Figure 18: Multiple Nucleotide Sequence Alignment. Nucleotide sequences for aRM101, aRM118, and aRM129 were aligned with wild type Alpha ENaC sequence. The wild type sequence was used from the PubMed database. The asterisk beneath each position signifies homology between sequences. Silent point mutations are highlighted in colors corresponding to the sample they are contained within. Point mutations resulting in a change in amino acid are highlighted in colors corresponding to the sample, bold, and underlined. Alignment was generated using Clustal Omega.

Alpha random mutant 101 contains three silent mutations and a single point mutation of a thymine substitution for an adenine resulting in the single amino acid change seen in the protein sequence. Alpha random mutant 118 has three silent mutations and a single point mutation of an adenine substitution for a thymine resulting in the single amino acid change seen in the protein sequence. Alpha random mutant 129 has two silent mutations and a single point mutation of a guanine substituted for an adenine resulting in the single amino acid change seen in the protein sequence.

Multiple Species Protein Alignment-Conserved Regions

An alignment of alpha ENaC protein sequences from multiple species was created using the Clustal Omega software (Figure 19). The positions of the amino acid changes in mutants 101, 118, and 129 were identified in the multiple species alignment to see if they were conserved, or occurred in conserved regions.

Figure 19: Multiple Species Alpha ENaC Protein Sequence Alignment. Alpha ENaC protein sequences in multiple species alignment using Clustal Omega. The asterisk beneath each position signifies homology between sequences. Mutant amino acid changes are highlighted in red. Yellow highlighting denotes the location of aRM101 mutation. Green highlighting denotes the location of aRM118 mutation. Blue highlighting denotes the location of aRM129 mutation.

All mutant positions fell within highly conserved regions. Alpha random mutant 101's amino acid change (N339I) fell within a position that is conserved within all aligned species except for *Xenopus laevis* (N/D). Alpha random mutant 118's amino acid change (L414H) fell within a position that is completely conserved within all aligned species (L). Alpha random mutant 129's amino acid change (D239G) fell within a position that is highly conserved except for *Xenopus laevis* and *Gallus gallus* which both contain the same amino acid difference from the other species represented (D/E).

Mutant Positions in Proposed ENaC Structure

Once nucleotide and amino acid changes were identified and their positions within conserved regions confirmed, the position of the mutations within the proposed ENaC structure were identified using Figure 20. Knowing the position of the mutations within the three dimensional structure of the extracellular loop could prove helpful in understanding the effect of the mutations on the function of the protein. The protein alignments in Figure 16 were compared to alignments in Figure 19A to identify which region of the extracellular loop the mutations occur in.

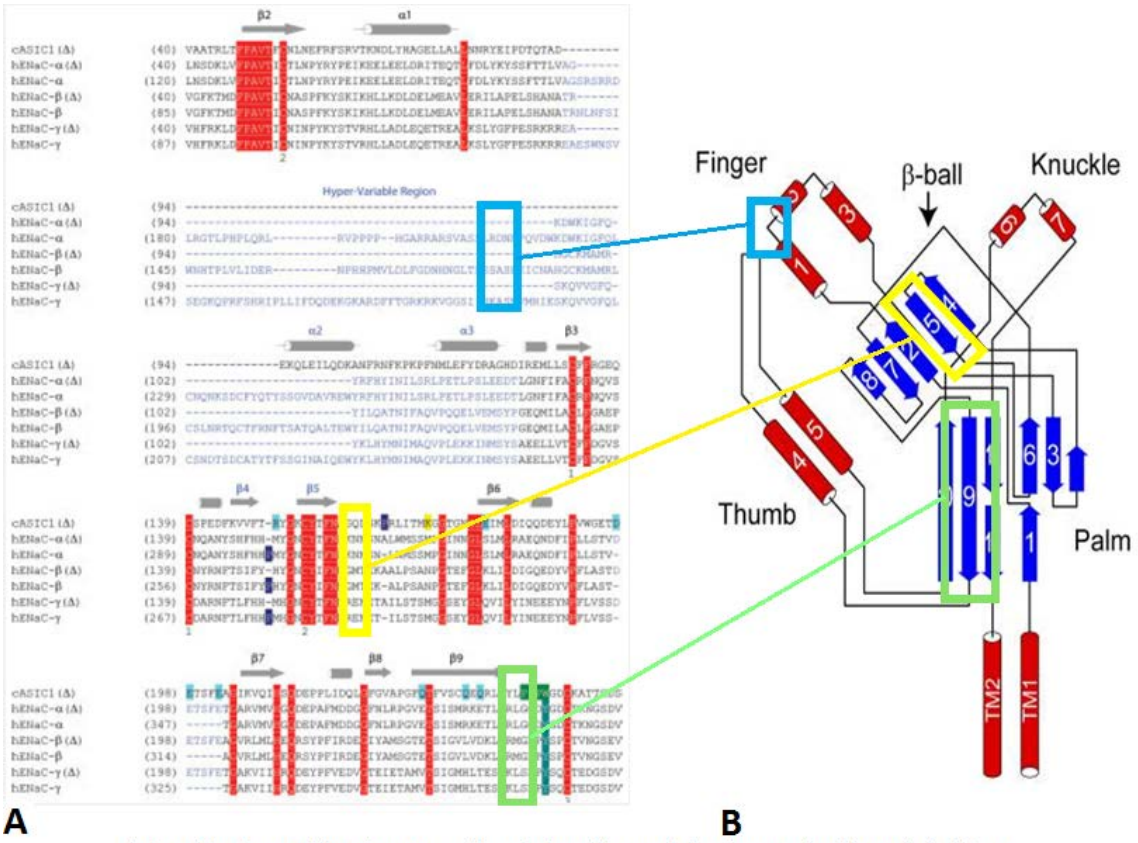

(A): Stockand, J. *et al.* (2008) IUBMB Life. 60 (B): Kashlan *et al.* (2011) Am J Physiol Renal Physiol. 301

Figure20: Proposed ENaC Subunit Structure. (A) Sequence alignment of ASIC1 with human alpha, beta, and gamma ENaC subunits proposed by Stockand Lab (10). (B) Predicted structure for human alpha ENaC subunit (2).

The substitution in alpha random mutant 101 is found within the β5 pleated sheet of the beta ball. Alpha random mutant 118 is found in the β9 pleated sheet of the palm region. The change in alpha random mutant 129 is found within the hyper-variable region between the α1 and α2 helices within the finger region. Although random mutant 129 falls within a hyper-variable region of human ENaC in comparison to ASIC1, it is still contained in a highly conserved region between ENaC sequences of different species (Figure 20).

Confirmation of Mutant αENaC Function in Yeast

To verify that results from the pronging assays were accurate and reproducible, a second transformation of αRM 101, 118, and 129 was conducted two months later. The protocols for transformation and pronging assays were not changed from that for the first transformation.

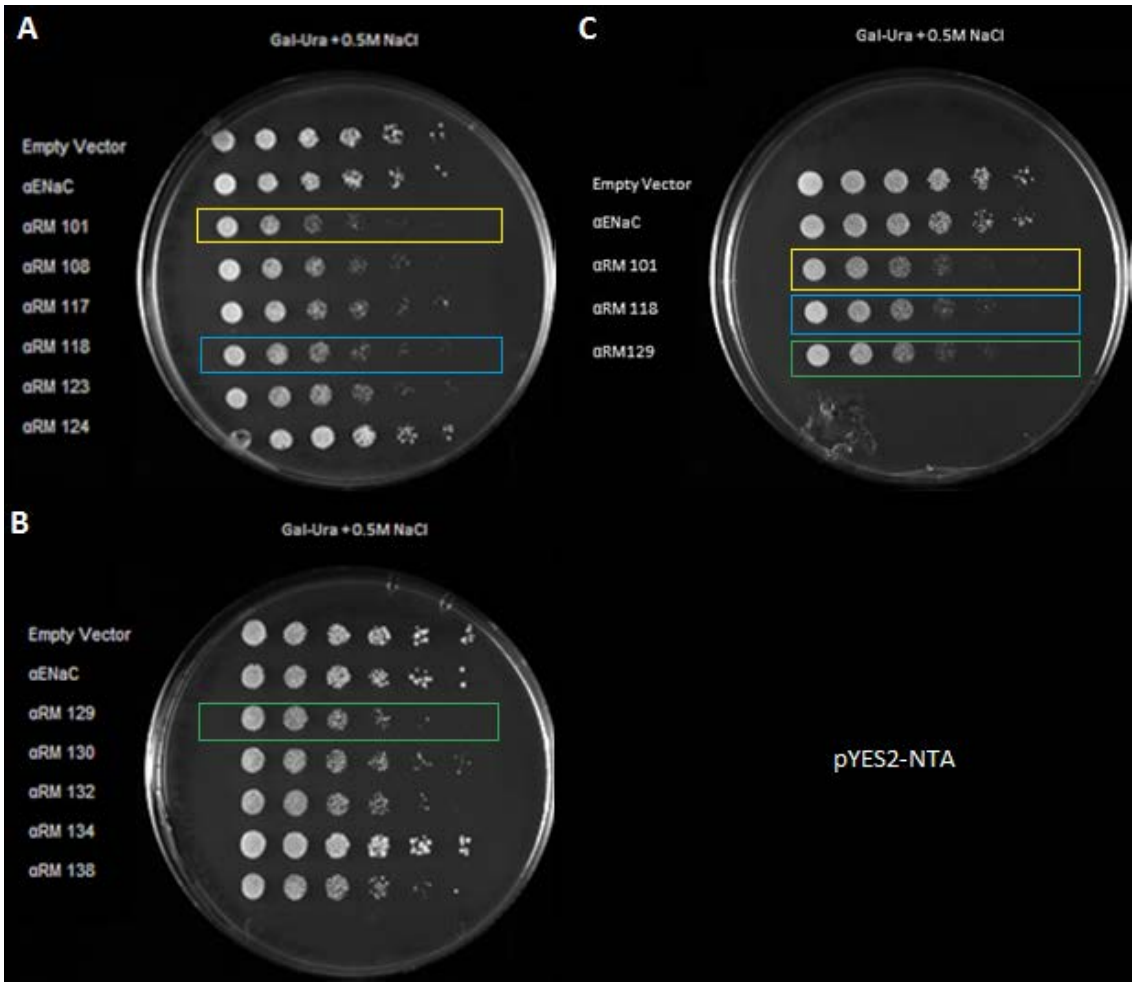

Figure 21: Comparison of pYES2-NTA Pronging Results for Transformations 1 and 2. (A, B) Alpha random mutant pronging for first transformation. (A) n=4, 72 hrs. (B) n=4, 96 hrs. (C) Alpha random mutant pronging for second transformation. (n=1, 72 hrs).

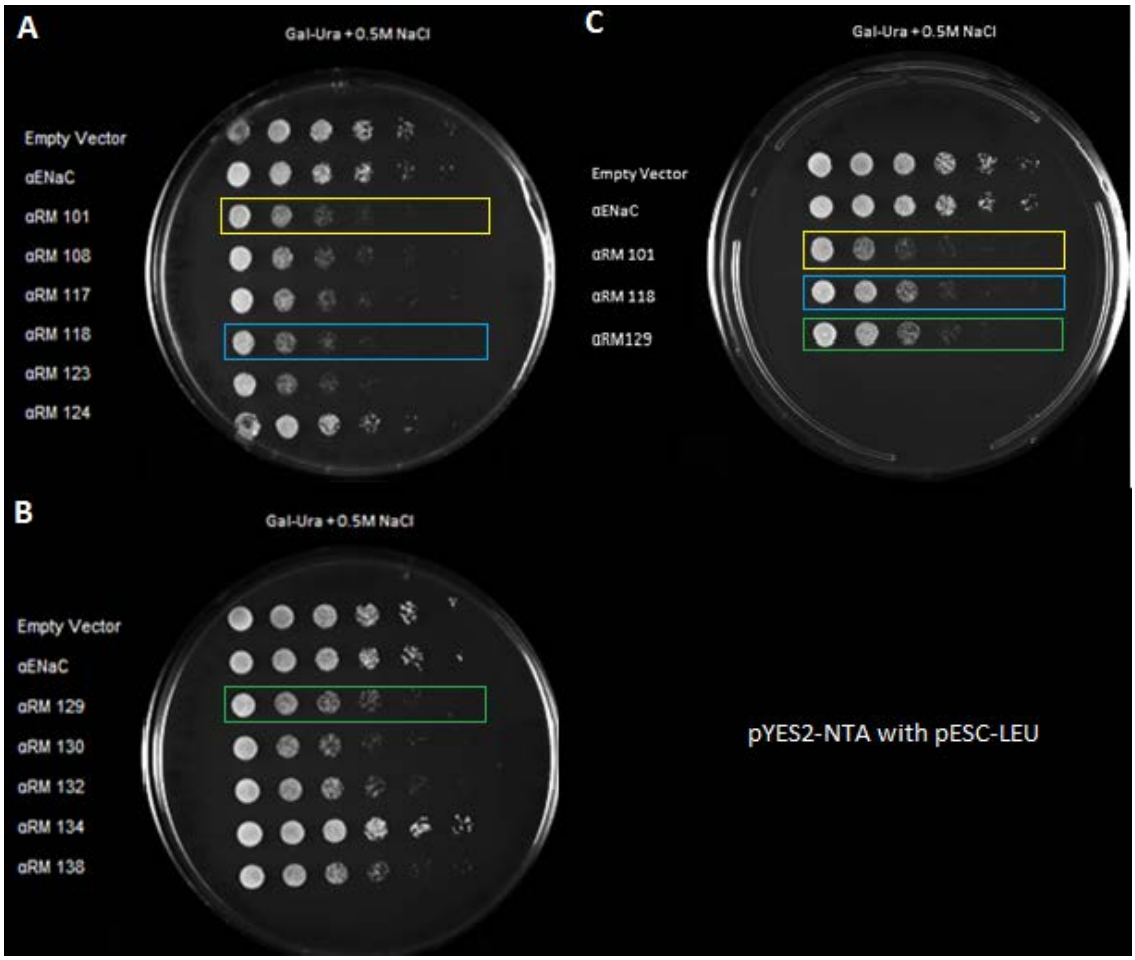

Figure 22: Comparison of pYES2-NTA/pESC-LEU Pronging Results for Transformations 1 and 2. (A, B) Alpha random mutant pronging for first transformation. (A) n=3, 72 hrs. (B) n=3, 96 hrs. (C) Alpha random mutant pronging for second transformation. (n=1, 72 hrs.)

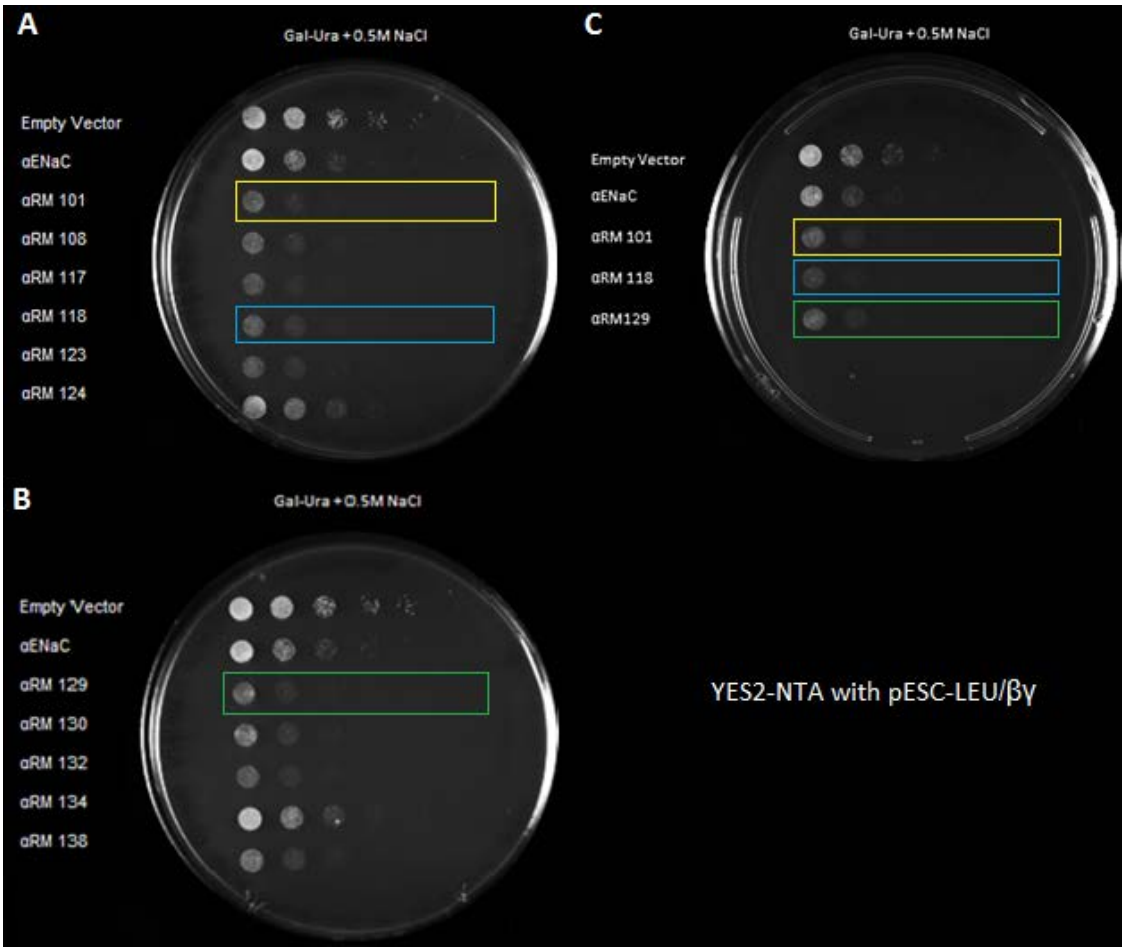

Figure 23: Comparison of pYES2-NTA Pronging Results for Transformations 1 and 2. (A, B) Alpha random mutant pronging for first transformation. (A) n=3, 96 hrs. (B) n=3, 96 hrs. (C) Alpha random mutant pronging for second transformation. (n=1, 72 hrs.)

The functionality of alpha random mutants 101, 118, and 129 were consistent between the first and second transformation prongings for the pYES2-NTA vector (Figure 21). In the pYES2-NTA with pESC-LEU vectors the mutants showed similar functional trends between both sets of pronging assays (Figure 22). The functionality of the mutants in the pYES2-NTA and the pYES2-NTA with pESC-LEU prongings for both transformations also showed consistency with one another which was expected as the addition of the empty pESC-LEU vector should not have affected αENaC

functionality in these homomeric channels (Figures 21 and 22). The functional trends in the pYES2-NTA with ESC-LEU/βγENaC were also consistent between prongings of the first and second transformations (Figure 23). These pronging comparisons show that the functionality changes observed within the alpha mutants are consistent, repeatable, and reliable.

Confirmation of ENaC Expression

Protein Expression

To confirm the expression of mutant alpha ENaC in yeast samples, yeast cultures were harvested from fresh patch plates and inoculated in 15 mL selective media (2% glu-ura for homomeric channels, and 2% glu-leu-ura for heteromeric channels) and grown 12-24 hours at 30°C with shaking. Cells were washed with expression media (2% gal-ura for homomeric channels, and 2% gal-leu-ura for heteromeric channels), centrifuged 1,500 x g for 5 minutes at 4°C, and then re-suspended in 50 mL expression media. Expression cultures were grown for 8 hours, 50 mL cultures were split into two 25 mL aliquots, and centrifuged at 1,500 x g for 5 minutes at 4°C.

Protein was extracted from one 25 mL aliquot of each sample using a post alkaline lysis protocol. Protein was extracted from the second 25 mL aliquot of each sample using an acid washed bead lysis protocol.

Lysates from the acid washed bead protein extraction were run in a BCA assay to quantitate concentration of total protein. These absorbances were used to create an average standard curve for the standard dilution using Microsoft Excel. The equation for

the slope of the line was used along with average absorbance values for each lysate sample to calculate the total protein concentration for each sample.

Lysates from the acid washed bead protein extractions were prepped for SDS-PAGE gel electrophoresis by combining 75 μg total protein with 1X NuPAGE LDS sample buffer and 2.5% v/v 2-mercaptoethanol. Samples were incubated at 95°C for 5 minutes before loading into polyacrylamide gels. Lysates from the post alkaline protein extraction were added directly to gels in 10 μL aliquots. Samples were loaded in SDS PAGE gels and separation by electrophoresis was conducted at 100 V for 70 minutes. PageRuler Plus pre-stained ladder was used as a standard.

Protein from SDS PAGE gels was transferred to nitrocellulose using the Trans-Blot Turbo™ RTA Transfer Kit following the manufacturer's protocol. Primary antibody, anti-Xpress, was added to each blot (1/5,000 dilution) and incubated 12-16 hours at 4°C with shaking. The primary antibody was removed and blots were washed in 20 mL TBST for five minutes three times each. Secondary antibody, anti-mouse (1/20,000 dilution), was added to the blots and agitated on a rocker for one hour. Blots were rinsed in 20 mL TBST three times for five minutes. A final rinse in 20 ml 1X TBS for 5 minutes followed. Western Lightning® Plus-ECL reagents were used to detect ENaC. Five long exposure images were taken in succession; one image every minute, for 5 minutes. A custom image setting allowed an image of the blot lacking luminescence to visualize the ladder. The software was used to merge these images to allow visualization of protein bands and standard ladder together.

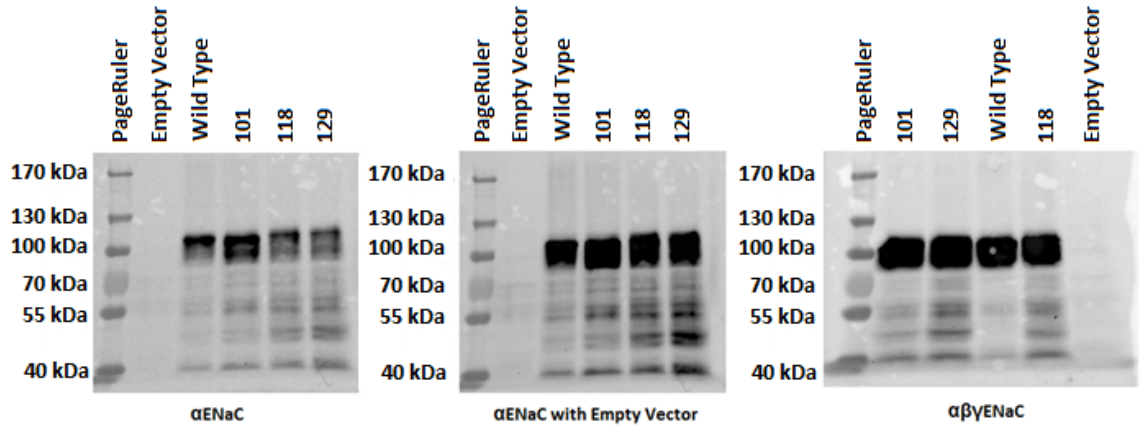

Figure 24: Acid Washed Bead Protein Extraction Western Blot with Anti-Xpress. All samples were visualized using Anti-Xpress primary antibody and Anti-Mouse secondary antibody.

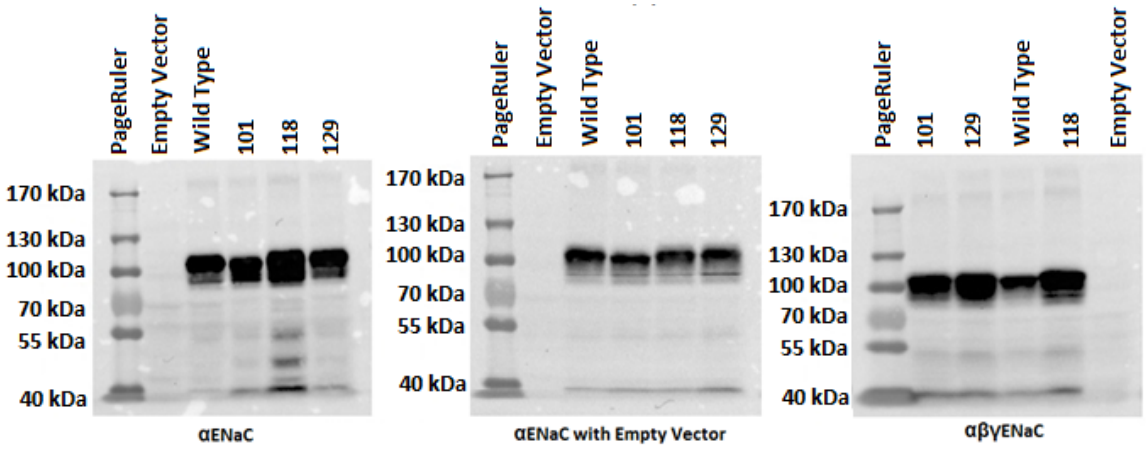

Figure 25: Post Alkaline Protein Extraction Western Blot with Anti-Xpress. All samples were visualized using Anti-Xpress primary antibody and Anti-Mouse secondary

All blots show no ENaC expression in negative controls (Figures 24 and 25, lanes 2, 8, and 18). All wild type alpha and alpha random mutant samples show the presence of alpha ENaC (Figures 24 and 25, all lanes excluding 1, 7, and 13). Alpha ENaC is visualized in each sample as a doublet. The higher molecular weight protein band signifies the protein in its glycosylated form. The lower molecular weight protein band signifies the protein that is un-glycosylated.

Antibody Stripping

Anti-Alpha

In order to probe the same blots with a different primary antibody they were subjected to a stripping protocol. All blots were stripped of Anti-Xpress and re-probed with Anti-Alpha primary antibody (1/5,000 dilution). The Anti-Xpress antibody has an affinity for the Xpress epitope on the N-terminus of the expressed protein. The Anti-Alpha antibody has an affinity for the alpha ENaC subunit but specific binding sites are unknown. Probing with both antibodies allows for comparisons to be made. If the levels of protein from the same blot are highly variable in images from both antibodies then further investigations would be needed to assess the probability of subunit cleavage. The primary antibody was removed and blots were rinsed with 20 mL TBST for 5 minutes three times. The secondary Anti-Rabbit antibody (1/20,000 dilution) was added and incubated. The secondary antibody was discarded and blots were rinsed and imaged.

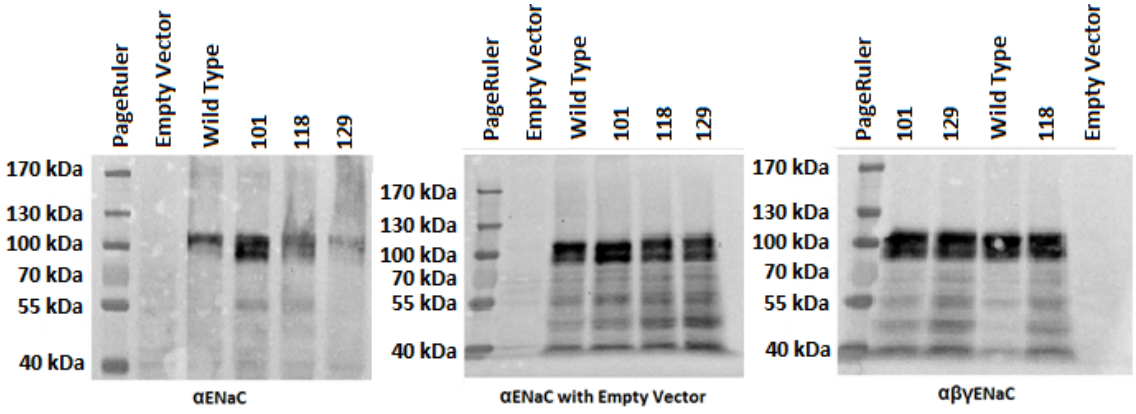

Figure 26: Acid Washed Bead Protein Extraction Western Blot with Anti-Alpha. All samples were visualized using Anti-Alpha primary antibody and Anti-Rabbit secondary.

Blots visualized using the Anti-Alpha antibody show detection of expressed alpha ENaC in each sample (Figure 26). There was no major difference between the

images of Anti-Alpha from that of Anti-Xpress suggesting that subunit cleavage is not of concern for these mutants.

Beta-Actin

Blots containing protein extracted through post alkaline lysis were stripped a second time and re-probed with beta-actin antibody. This antibody is HRP conjugated so only required a 1 hour incubation time (1/1,000 dilution).

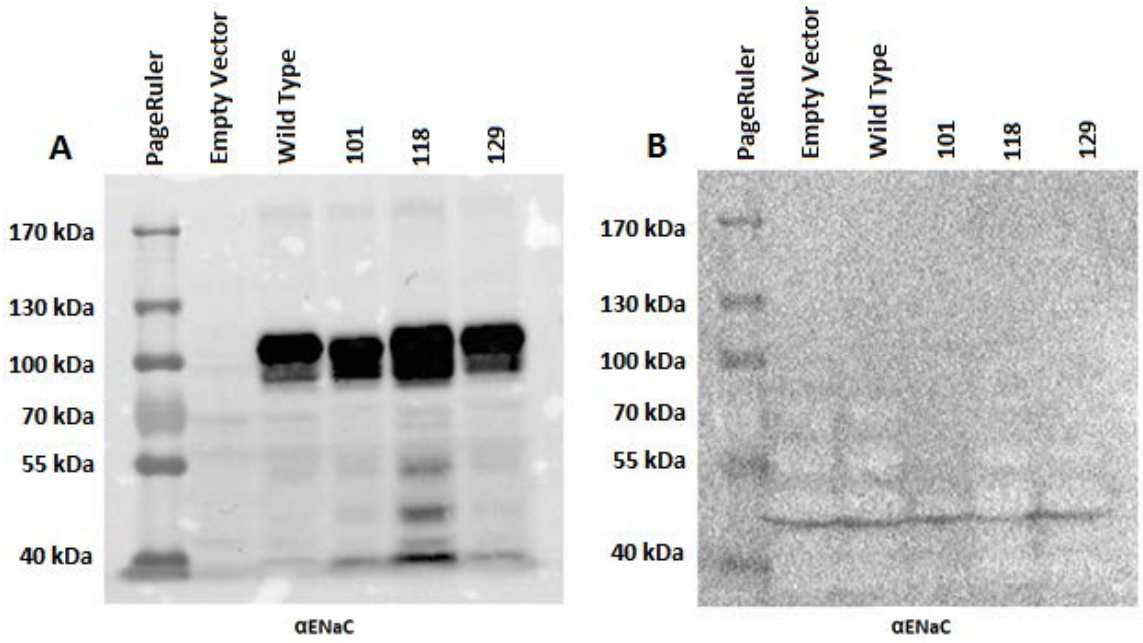

Figure 27: Alpha ENaC Post Alkaline Protein Extraction Western Blot Anti-Xpress Comparison with Anti Beta-Actin. (A) Post alkaline protein extraction lysates visualized with Anti-Xpress primary and Anti-Mouse secondary antibodies. (B) Stripped post alkaline protein extraction blot probed with HRP-conjugated Anti Beta-Actin antibody.

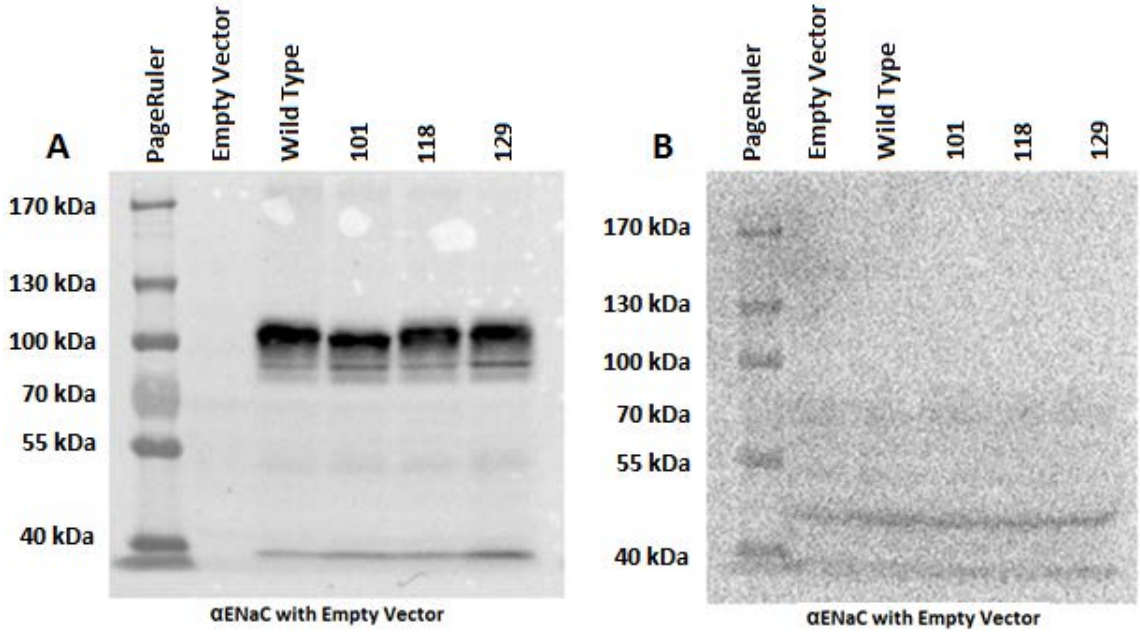

Figure 28: Alpha ENaC with Empty Vector Post Alkaline Protein Extraction Anti-Xpress Western Blot Comparison with Anti Beta-Actin. (A) Post alkaline protein extraction lysates visualized with Anti-Xpress primary and Anti-Mouse secondary antibodies. (B) Stripped post alkaline protein extraction blot probed with HRP-conjugated Anti Beta-Actin antibody.

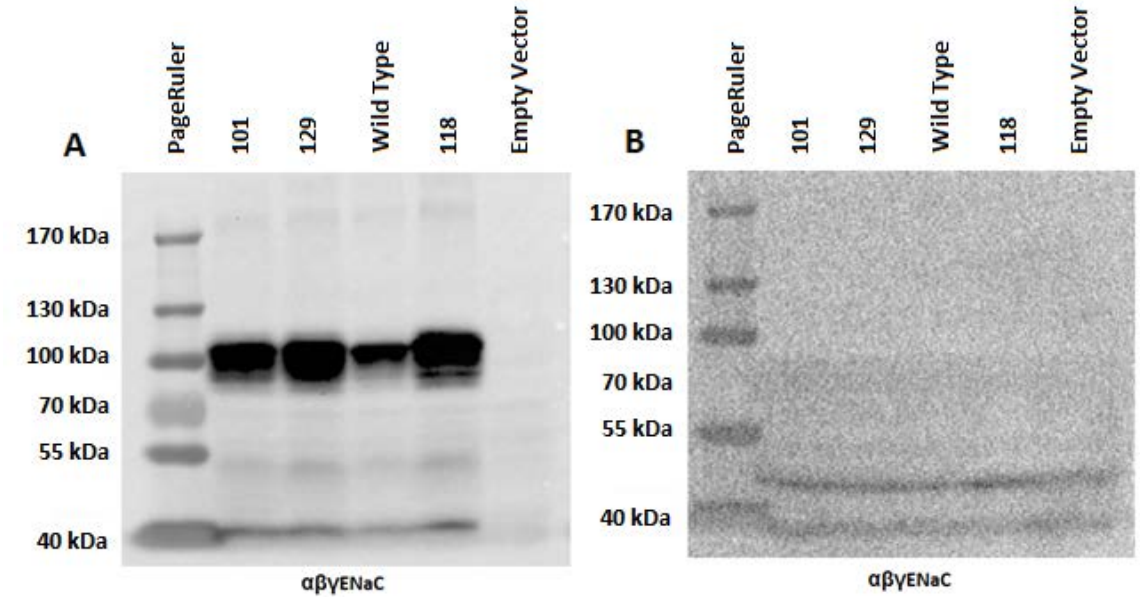

Figure 29: Alpha, Beta, Gamma ENaC Post Alkaline Protein Extraction Western Blot Anti-Xpress Comparison with Anti Beta-Actin. (A) Post alkaline protein extraction lysates visualized with Anti-Xpress primary and Anti-Mouse secondary antibodies. (B) Stripped post alkaline protein extraction blot probed with HRP-conjugated Anti Beta-Actin antibody.

The reagents used for post alkaline protein extraction make total protein quantification through BCA assay technically impossible. In its place the expression levels of beta actin were used as a loading control for each sample, therefore, ENaC protein band intensity relative to beta actin intensity can be used as an indication of expression levels. Beta actin bands in these blots show similar intensity between samples suggesting the intensity of the ENaC samples are representative of expression level when compared within the same blot (Figures 27, 28, and 29). However, the lack of separation between the protein bands in each beta actin sample compared to the Anti-Xpress visualization gave cause for concern. Exposure of the blots represented here allow for positive detection of the αENaC being expressed in each sample, but future investigations would be needed to accurately compare expression levels between samples.

Time Course Growth Assay

To test the effect of the alpha mutants on the growth rate of cells, samples were subjected to a time course study in the presence of 2% galactose and 0.5 M NaCl. Absorbances for each three hour time period were used to create a graph in Microsoft Excel (Figure 30) and growth rates were compared using the slope of the best fit line for each sample (Figure 31).

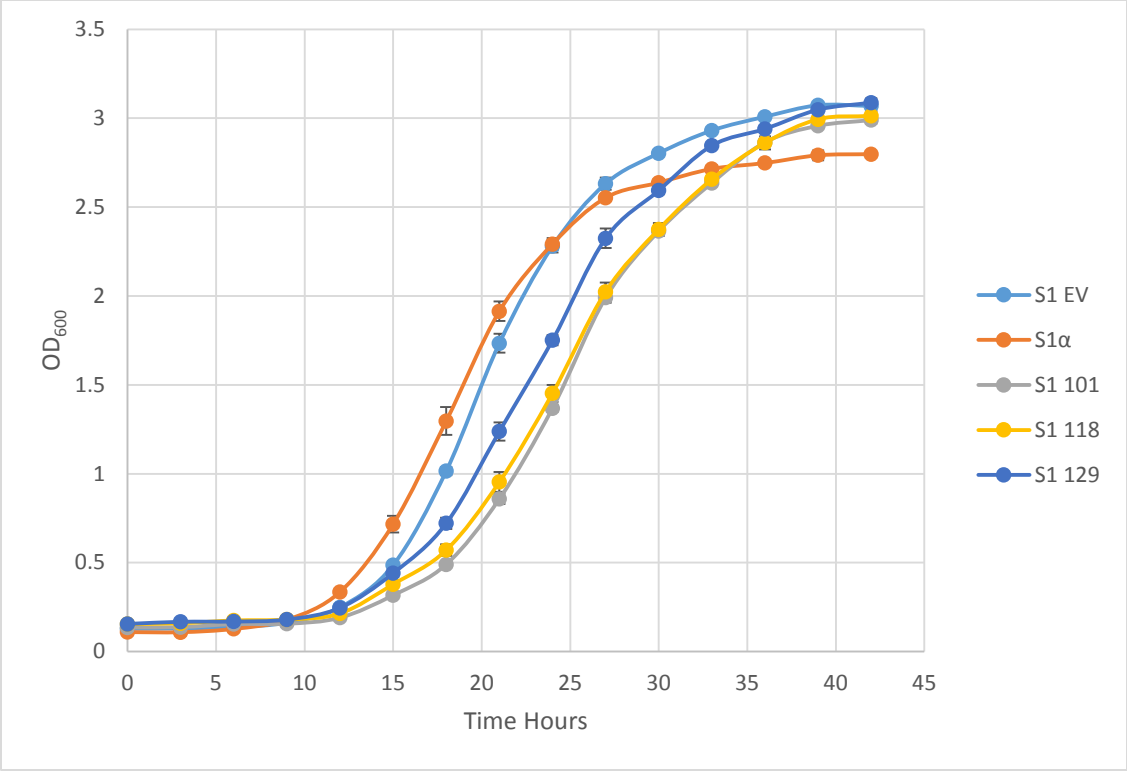

Figure 30: Alpha Random Mutant Time Course. Absorbances of *S. cerevisiae* cell cultures (n=2) transformed with empty vector pYES2-NTA, wild type αpYES2-NTA, αRM101pYES2-NTA, αRM118pYES2-NTA, and αRM129pYES2-NTA at three hour intervals. Curve represents lag, log, and stationary growth phases of each cell type in the presence of 0.5 M NaCl.

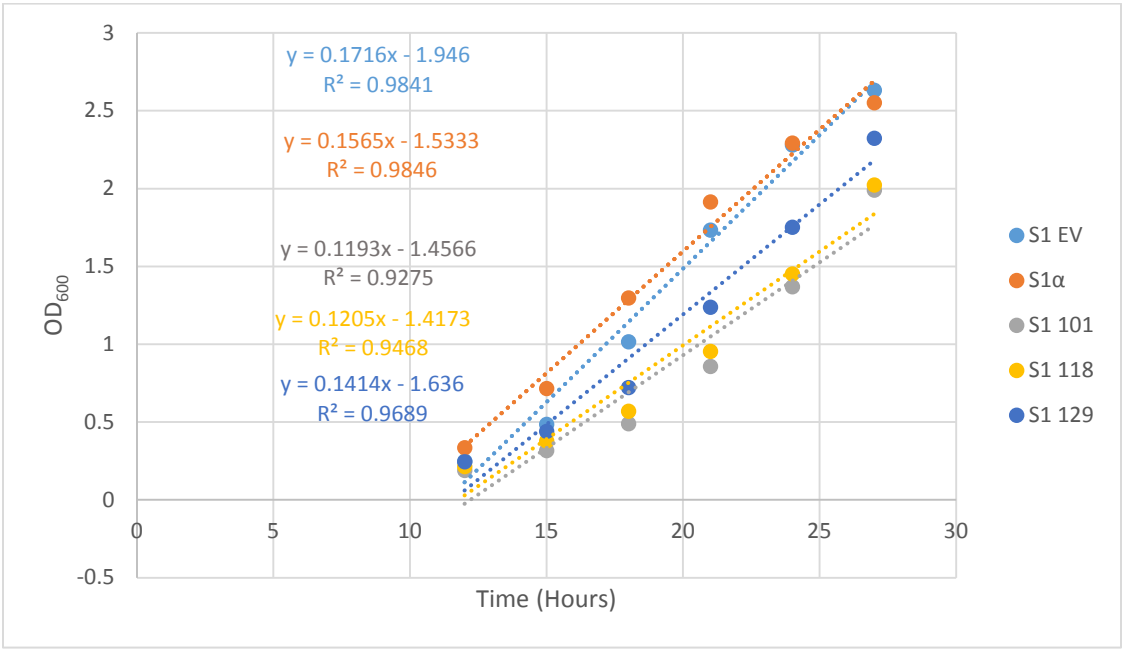

Figure 31: Alpha Random Mutant Time Course Log Phase Slope. Log phase absorbances were plotted independently and linear trend lines were generated. The slope of each trend line is shown to be used for comparison of growth rate during log phase.

The growth rate of cells was expected to be slower in samples expressing functional αENaC. The presence of the protein in the membrane allowed sodium to move into the cells causing lower survival which in turn resulted in a fewer amount of cells able to replicate. The slope of the empty vector cultures was greater than the cultures expressing αENaC (Figure 31). Based on the pronging studies all alpha random mutants showed lower cell survival indicating a more highly functional channel. Mutant cultures were expected to have lower growth rates than that of wild type αENaC. Alpha random mutants 101 and 118 had a smaller slope than wild type alpha as expected. Alpha random mutant 129 had a slope slightly higher than wild type which was unexpected (Figure 31). Duplicate trials containing 0.5 M NaCl and a time course containing no additional salt could be performed in the future for further clarification.

Mammalian Expression Studies

Once yeast functional screenings were completed the function of the alpha mutants in a mammalian system was examined. Dr. Nina Boiko at the University of Texas Health and Science Center in San Antonio, TX agreed to complete electrophysiological patch clamp studies on mammalian cells transfected with the alpha mutants. In order to complete these studies the alpha mutant genes needed to be cloned into a mammalian vector.

pCMV-Myc Mammalian Expression Vector

The pCMV-Myc mammalian expression vector (Figure 32) was previously cloned with alpha, beta, and gamma ENaC subunits individually by Dr. Rachell Booth.

The pCMV-Myc vector contains a selective marker for ampicillin resistance and the pUC origin of replication, both for use in bacterial cell lines. The vector allowed expression of proteins with an N-terminal immunoreactive c-Myc epitope tag which was utilized for protein detection in western blots.

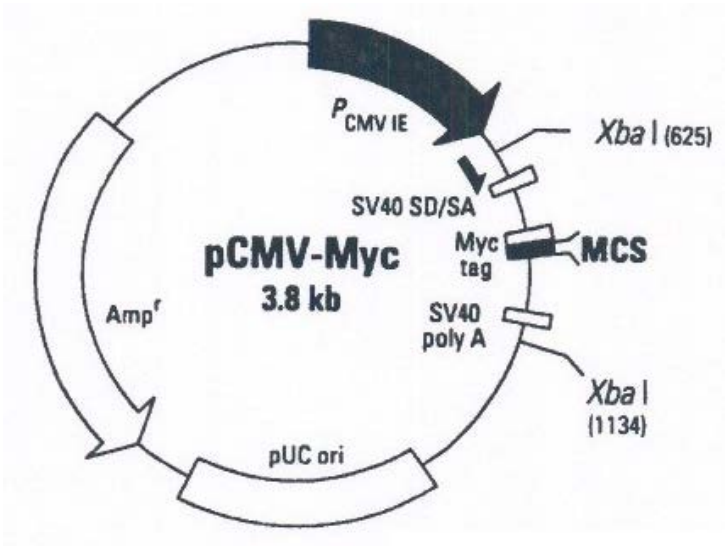

Figure 32: pCMV-Myc Expression Vector Map. The pCMV-Myc vector was cloned with wild type alpha ENaC and alpha random mutants 101, 118, and 129.

Alpha and Beta pCMV-Myc Sample Preparation

Our lab did not have a sample of empty pCMV-Myc so pCMV-Myc/βENaC was used as a source of the empty vector. The βENaC gene was slightly smaller than the αENaC gene, so use of pCMV-Myc/βENaC allowed confirmation of the alpha insert being cloned after ligation as the pCMV-Myc/αENaC samples would run slightly higher than pCMV-Myc/βENaC in an agarose gel. Alpha pCMV-Myc was used as a positive control. A personal stock of pCMV-Myc/αENaC and pCMV-Myc/βENaC was created by transforming plasmid into Top 10 *E. coli* using the KCM protocol. Isolated plasmid samples were analyzed through horizontal gel electrophoresis (Figure 33) to confirm the

presence of transformed plasmid. Daniel Horn's plasmid samples were used as positive controls.

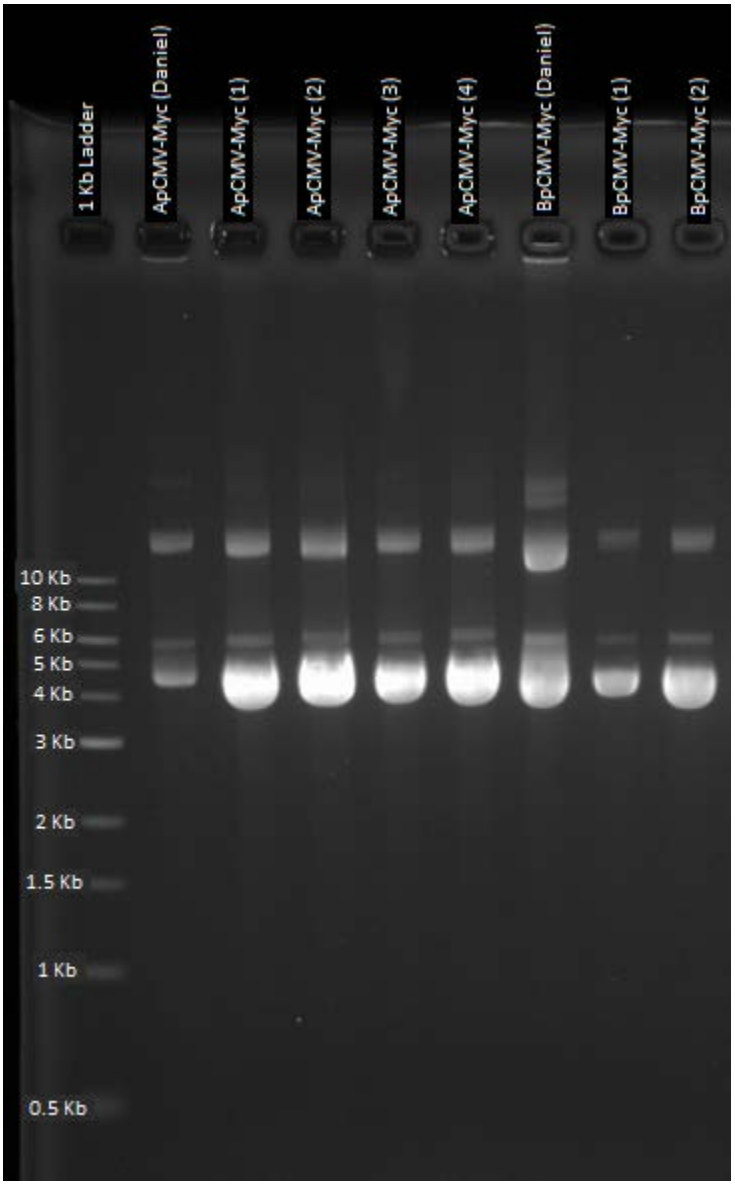

Figure 33: Confirmation of Transformed pCMV-Myc Samples. pCMV-Myc/αENaC and pCMV-Myc/β were transformed into *E. coli* to create personal plasmid stocks to be used for cloning. This gel confirms the presence of these plasmids in new *E. coli* stocks.

All selected colonies contained the necessary plasmid. Glycerol stocks were made for each transformed *E. coli* sample and stored at -80°C. Plasmids were stored at -20°C until further use.

Restriction Digest, Gel Extraction, and Purification

In order to isolate the empty pCMV-Myc vector from pCMV-Myc/βENaC and the alpha ENaC genes (wild type and mutants) from pYES2-NTA/αENaC, double digestion reactions were completed using EcoRI-HF and NotI-HF.

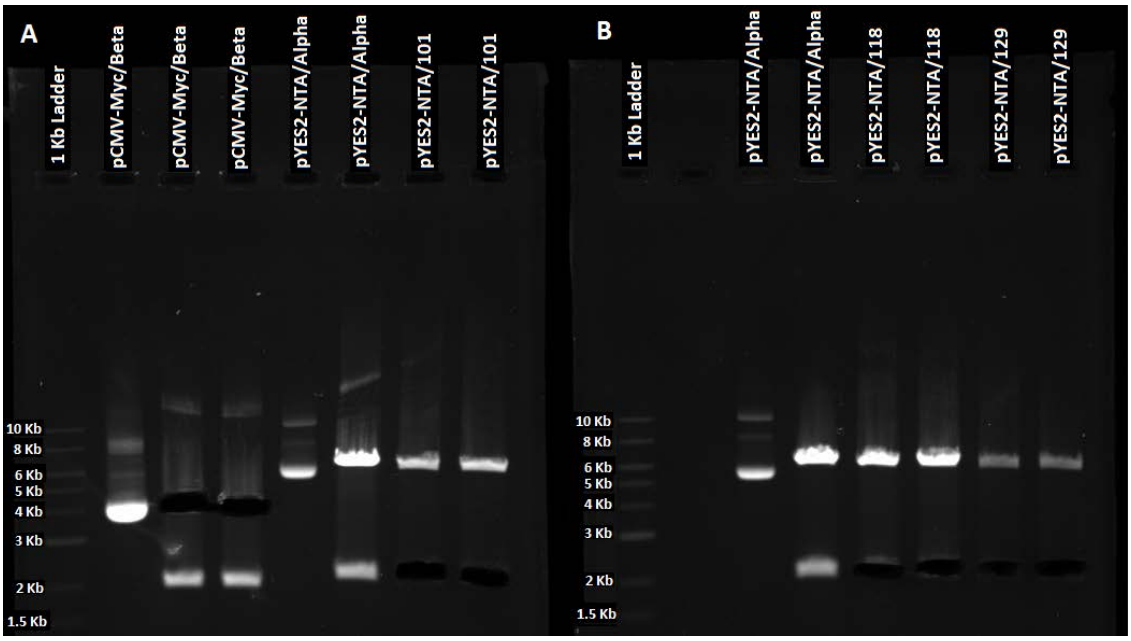

Figure 34: Vector and Insert Extraction from Agarose Gels. Empty pCMV-Myc vector and alpha ENaC gene inserts were extracted from restriction digest products of pCMV-Myc/βENaC and pYES2-NTA/αENaC samples. Two DNA fragments for each sample were extracted to increase amount of genetic material isolated.

Ligation

Ligation of the mutant ENaC genes with the pCMV-Myc vector was accomplished by setting up reactions with a 3:1 insert to vector ratio. The ligated solution was transformed into Top 10 *E. coli* cells using the KCM protocol and plated on LB-AMP plates. Two single colonies for each sample were selected from transformation plates, plasmid was isolated from overnight cultures, and concentrations quantified.

A new lab stock of competent Top 10 *E. coli* was used for above transformation. These cells proved to be inefficient so plasmid was transformed into a different Top 10 stock. The second set of cells was efficient, and plasmids isolated from the second transformation were stored at -20°C until further use.

Ligation Confirmation with Restriction Digest

Ligated plasmid DNA was subjected to a restriction digest with BamHI to confirm correct ligation. DNA fragments needed for identification were very small so the amount of plasmid DNA used in the following digestion was doubled from the regular 1 µg to approximately 2 µg. Reactions were analyzed by horizontal gel electrophoresis in a (Figure 35). The need for visualization of smaller DNA fragments required the use of a more concentrated agarose gel (1.5%) which in turn required longer running time.

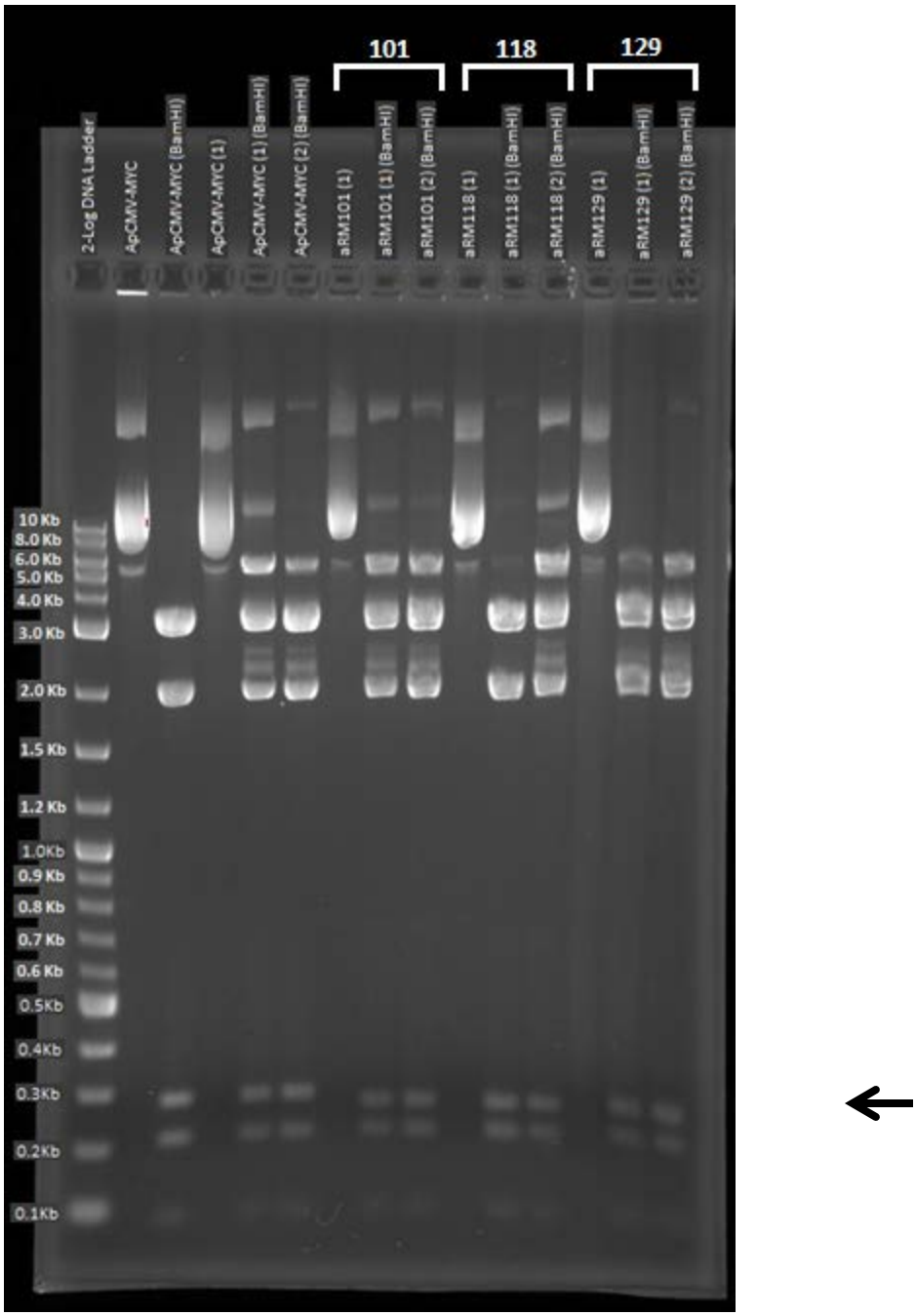

Figure 35: Confirmation of Ligation Reactions for Alpha pCMV-Myc Cloning. Plasmid samples from two colonies of each transformed ligation reaction and pCMV-Myc/αENaC controls were digested with BamHI to test for successful ligation of the alpha ENaC genes into the pCMV-Myc vector.

Restriction of pCMV-Myc/αENaC with BamHI as predicted by NEBcutter from New England Biolabs should result in five DNA fragments (approximately 3,300 bp,

2,000 bp, 270bp, 200 bp, and 80 bp). Restriction of pCMV-Myc/βENaC with BamHI should result in 4 DNA fragments (approximately 3,300 bp, 2,000 bp, 200 bp, and 80 bp). If cloning was successful restriction of each sample should result in full five DNA fragments. If cloning was unsuccessful and samples still contain the βENaC gene the restriction would contain only four DNA fragments. The DNA fragment of interest for identifying αENaC containing plasmids from beta containing plasmids was the ~270 bp DNA fragment. All samples contained this DNA fragment confirming successful ligation of the αENaC gene into the pCMV-Myc vector.

Isolating Plasmid Samples for Mammalian Studies

Once samples were confirmed 40 µg of plasmid DNA was needed to send to Dr. Boiko at the University of Texas Health and Science Center in San Antonio, TX (UTHSCSA) for mammalian transfection and electrophysiological studies. Plasmid was isolated from transformed *E. coli* for each mutant using Qiagen QIAprep Spin Miniprep kit. Upon receiving the plasmids Dr. Boiko transformed them into Top 10 *E. coli* cells and isolated plasmid utilizing endotoxin free midi prep. Plasmids were then transfected into Chinese hamster ovary (CHO) cells and grown on glass chips for use in electrophysiology studies.

Electrophysiology Patch Clamp Studies

To conduct electrophysiology studies plasmids were transfected into Chinese hamster ovary (CHO) cells and grown on glass chips. CHO cells were used for this

study because they do not endogenously express any other sodium channels. Dr. Boiko conducted patch clamping studies on non-transfected CHO cells as well as cells transfected with wild type αENaC and all alpha random mutant ENaCs. She collected data from at least three cells per transfection from three separate transfections (n=10) and compiled data to compare functionality of mutant ENaC channels to wild type ENaC based on their current (Figure 36).

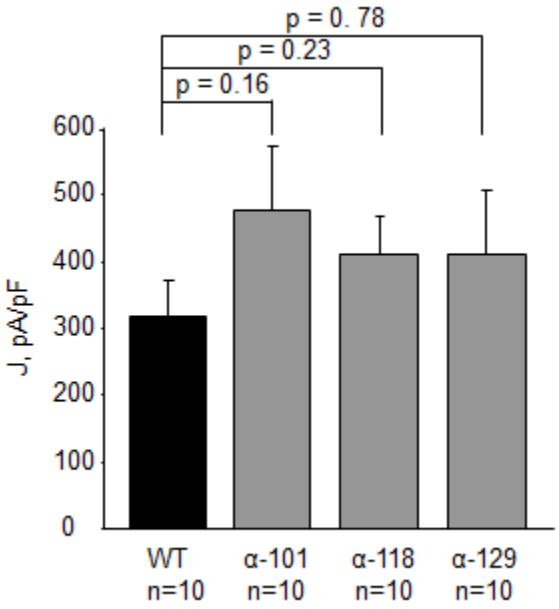

Figure 36: mENaC-Myc Expressed in CHO (0.3µg α, 0.3µg β, and 0.3µg γ). Sodium currents observed in patch clamp studies of mutant pCMV-Myc/αENaC in CHO cells.

Preliminary data shows a trend of slightly increased currents in cells expressing the mutant αENaCs when compared to wild type, but none are of statistical significance. Dr. Boiko has agreed to continue the study by increasing the number of replicates to assess if the changes in current are of statistical significance in a larger sample size.

Mammalian Western Blots

Dr. Boiko grew CHO cells transfected with wild type and mutant ENaC to be used for protein detection through western blotting. Patch clamping studies at UTHSCSA were observed, and protein was extracted from transfected cells using the mammalian cell protocol. Cell lysates were subjected to a BCA assay to quantify total protein concentrations using the same protocol used for yeast cell lysates. Lysates were prepped and analyzed by SDS-PAGE gel electrophoresis.

Protein from the gel was transferred to a nitrocellulose membrane utilizing the TransBlot system as before for yeast blots. Anti-Myc primary antibody was used for visualization of protein (Figure 37).

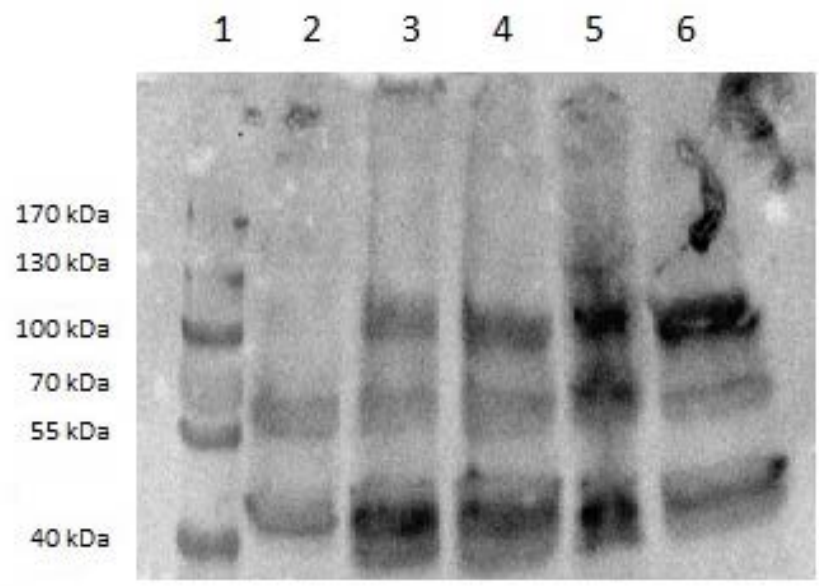

Figure 37: CHO Cell Protein Extraction Anti-Myc Western Blot. (1) PageRuler Plus pre-stained ladder used as a standard. (2) Non-transfected CHO cell lysate. (3) pCMV-Myc/αENaC CHO cell lysate. (4) pCMV-Myc/aRM101ENaC CHO cell lysate. (5) pCMV-Myc/aRM118ENaC CHO cell lysate. (6) pCMV-Myc/aRM129ENaC CHO cell lysate.

Transfected cell samples all showed detection of expressed ENaC protein while non-transfected sample lysate showed no ENaC expression as expected.

IV. CONCLUSIONS

Within the ENaC/DEG superfamily of ion channels the greatest genetic variability is found within the extracellular loop domain. There is very limited knowledge of the functional importance of specific residues within this region of ENaC. Mutations induced in the extracellular loop of the alpha ENaC subunit were successfully characterized through serial dilution survival assays utilizing *Saccharomyces cerevisiae* yeast strain S1InsE4A. Mutations causing increased ENaC function suggested lower cell survival while mutations causing decreased ENaC function suggested increased cell survival compared to wild type ENaC. Changes in functionality were supported by further examination of mutant ENaCs through growth curve analysis which showed a decrease in log phase growth rate in cells expressing ENaC and ENaC mutants when compared to cells transformed with an empty vector. Western blotting was utilized to confirm expression of ENaC within transformed yeast cells and gave preliminary insight on differences in expression levels based on amino acid changes. This quick screen for critical residues in ENaC using yeast allows for a fast, inexpensive examination of the functional effect of mutations.

Three single amino acid changes were identified in yeast screens as causing an increase in functionality of ENaC; (1) alpha random mutant 101 (N340I), (2) alpha random mutant 118 (L415H), and (3) alpha random mutant 129 (D240G). Each amino acid change caused a change in chemical property of the residue present. This change in chemical property may be causing repulsion of residues resulting in a widening of the extracellular loop domains above the pore or even the pore itself. This increase in size

may lead to the increased functionality of the mutants by allowing better access to the pore or a greater number of sodium ions being able to pass through the protein complex at once. Sequence analysis showed that these residues fall within conserved regions of ENaC when aligned with several species, also supporting the importance of these residues for ENaC function.

For further functional testing, alpha random mutants 101, 118, and 129 were cloned into the mammalian vector pCMV-Myc and sent to collaborators at the University of Texas Health and Science Center in San Antonio, TX for electrophysiological patch clamp studies in Chinese hamster ovary cells. These studies quantified the change in current produced between mutant and wild type ENaC in heteromeric channels. While there was some evidence of increased currents with the mutant ENaCs, none were of statistical significance in preliminary testing.

Future studies should be conducted to further elucidate the effects of these mutations within mammalian and yeast systems. Similar screening studies in both model systems could also be conducted to identify other residues of critical importance within the extracellular loop. Compiling this data into an amino acid map of the extracellular loop could prove helpful in identifying each residue that is critical for optimal function of the alpha ENaC subunit.

LITERATURE CITED

1. Garty, H. Molecular properties of epithelial, amiloride-blockable Na^+ channel. *The FASEB Journal.* (1994) 8: 522-528
2. Kashlan, O. B., and Kleyman, T. R. ENaC structure and function in the wake of resolved structure of a family member. *Am J Renal Physiol*. (2011) 301: F684-F696
3. Rossier, B. C. Epithelial sodium channel (ENaC) and the control of blood pressure. *Current Opinion in Pharmacology*. (2014) 15: 33-46
4. Mozaffarian, D., et al. Heart disease and stroke statistics-2015 update: A report from the American Heart Association. *Circulation*. (2015) 131:e29-e322
5. Bahalla, V., and Hallows, K. R. Mechanisms of ENaC regulation and clinical implications. *J Am Soc Nephrol.* (2008) 19:1845-1854.
6. Snyder, P. M. The epithelial Na^+ channel: Cell surface insertion and retrieval in Na^+ homeostasis and Hypertension. *Endocrine Reviews*. (2002) 23(2):258-275
7. Kellenberger, S., and Schild, L. Epithelial sodium channel/degenerin family of ion channels: A variety of Functions for a Shared Structure. *Physiol Rev*. (2002) 82: 735-767
8. Markin, V. S., and Martinac, B. Mechanosensitive ion channels as reporters of bilayer expansion: A theoretical model. *Biophys. J*. (1991) 60: 1120-1127
9. Hamm, L. L., MD, Feng, Z, MD, and Hering-Smith, K. S., MS, PhD. Regulation of sodium transport by ENaC in the kidney. http://www.ncbi.nlm.nih.gov/pmc/articles/PMC2895494
10. Stockand, J. D., Staruschenko, A., Pochynyuk, O., Booth, R. E., and Silverton, D. U. Insight toward epithelial Na^+ channel mechanism revealed by the acid-sensing ion channel 1 structure. *Life*. (2008) 60(9): 620-628
11. Strauschenko, A., Adams, E., Booth, R. E., and Stockand, J. D. Epithelial Na+ channel subunit stoichiometry. *Biophysical Journal*. (2005) 88: 3966-3975
12. Bonny, O., Chraibi, A., Loffing, J., Jaeger, N. F., Gründer, S., Horisberger, J. D., and Rossier, B. C. Functional expression of pseudohypoaldosteronism type I mutated epithelial Na^+ channel lacking the pore-for minutesg region of its α subunit. *The Journal of Clinical Investigation.* (1999) 104(7): 967-974
13. Canessa, C. M., Schild, L., Buell, G., Thorens, B., Gautschi, I., Horisberger, J. D., and Rossier, B. C. Amiloride-sensitive epithelial Na^+ channel is made of three homologous subunits. *Nature* (1994) 367: 463-467

14. Firsov, D., Gautschi, I., Merillat, A. M., Rossier, B. C., and Schild, L. The heterotetrameric architecture of the epithelial sodium channel (ENaC). *The EMBO Journal*. (1998) 17(2): 344-352
15. Jasti, J., Furukawa, H., Gonzales, E. B., and Gouaux, E. Structure of acid-sensing ion channel 1 at 1.9 Å resolution and low pH. *Nature*. (2007) 449: 316-323
16. Kleyman, T. R., Carattino, M. D., and Hughey, R. P. ENaC at the cutting edge: Regulation of epithelial sodium channels by proteases. *Journal of Biological Chemistry*. (2009) 284(31): 20447-20451
17. Butterworth, M. B.., Weisz, O. A., and Johnson, J. P. Some assembly required: Putting the epithelial sodium channel together. *Journal of Biological Chemistry*. (2008) 283(51): 35305-35309
18. Mano, I., and Driscoll, M. DEG/ENaC channels: a touchy superfamily that watches its salt. *Bioessays*. (1999) 21: 568-578
19. Yang, K. Q., Xiao, Y., Tian, T., Gao, L. G., and Zhou, X. L. Molecular genetics of Liddle's syndrome. *Clinica Chimica Acta*. (2014) 436: 202-206
20. Shimkets, R. A. et. al. Little's syndrome: Heritable human hypertension caused by mutations in the β subunit of the epithelial sodium channel. *Cell*. (1994) 79(3): 407-414
21. Hansson, J. H., Nelson-Williams, C., Suzuki, H., Schild, L., Shimkets, R., Lu, Y., Canessa, C., Iwasaki, T., Rossier, B., and Lifton, R.P. Hypertension caused by a truncated epithelial sodium channel γ subunit: Genetic heterogeneity of Liddle syndrome. *Nature Genetics*. (1995) 11: 76-82
22. Pradervand, S., Vandewalle, A., Bens, M., Gautschi, I., Loffing, J., Hummler, E., Schild, L. and Rossier, B. C. Dysfunction of the epithelial sodium channel expressed in the kidney of a mouse model for Liddle syndrome. *J Am Soc Nephro*. (2003) 14: 2219-2228
23. Hummler, E., and Horisberger, J. D. Genetic disorders of membrane transport V. The epithelial sodium channel and its implication in human diseases. *Am J Physiol* 276 (Gastrointest. Liver Physiol. 39). (1999) G567-G571